Bioorg. Med. Chem. 32 (2021) 116014

Contents lists available at ScienceDirect

Bioorganic & Medicinal Chemistry

journal homepage: www.elsevier.com/locate/bmc

Synthesis, anticancer activity and molecular docking studies of *N*-deacetylthiocolchicine and 4-iodo-*N*-deacetylthiocolchicine derivatives

Greta Klejborowska [a], Alicja Urbaniak [b], Ewa Maj [c], Joanna Wietrzyk [c], Mahshad Moshari [d], Jordane Preto [e], Jack A. Tuszynski [e,f], Timothy C. Chambers [b], Adam Huczyński [a,*]

[a] Department of Medical Chemistry, Faculty of Chemistry, Adam Mickiewicz University, Uniwersytetu Poznańskiego 8, 61-614 Poznan, Poland
[b] Department of Biochemistry and Molecular Biology, University of Arkansas for Medical Sciences, Little Rock, AR 72205, United States
[c] Hirszfeld Institute of Immunology and Experimental Therapy, Polish Academy of Sciences, Rudolfa Weigla 12, 53-114 Wrocław, Poland
[d] Depertment of Chemistry, University of Alberta, Edmonton, Alberta T6G 1Z2, Canada
[e] Depertment of Oncology, University of Alberta, Edmonton, Alberta T6G 1Z2, Canada
[f] DIMEAS, Politecnico di Torino, Corso Duca degli Abruzzi 24, Turin, Italy

ARTICLE INFO

Keywords:
Colchicine binding site inhibitor
Antimitotic agent
Antiproliferative activity
Thiocolchicine

ABSTRACT

Colchicine is a plant alkaloid with a broad spectrum of biological and pharmacological properties. It has found application as an anti-inflammatory agent and also shows anticancer effects through its ability to destabilize microtubules by preventing tubulin dimers from polymerizing leading to mitotic death. However, adverse side effects have so far restricted its use in cancer therapy. This has led to renewed efforts to identify less toxic derivatives. In this article, we describe the synthesis of a set of novel double- and triple-modified colchicine derivatives. These derivatives were tested against primary acute lymphoblastic leukemia (ALL-5) cells and several established cancer cell lines including A549, MCF-7, LoVo and LoVo/DX. The novel derivatives were active in the low nanomolar range, with 7-deacetyl-10-thiocolchicine analogues more potent towards ALL-5 cells while 4-iodo-7-deacetyl-10-thiocolchicine analogues slightly more effective towards the LoVo cell line. Moreover, most of the synthesized compounds showed a favorable selectivity index (SI), particularly for ALL-5 and LoVo cell lines. Cell cycle analysis of the most potent molecules on ALL-5 and MCF-7 cell lines revealed contrasting effects, where M-phase arrest was observed in MCF-7 cells but not in ALL-5 cells. Molecular docking studies of all derivatives to the colchicine-binding site were performed and it was found that five of the derivatives showed strong β-tubulin binding energies, lower than −8.70 kcal/mol, while the binding energy calculated for colchicine is −8.09 kcal/mol. The present results indicate that 7-deacetyl-10-thiocolchicine and 4-iodo-7-deacetyl-10-thiocolchicine analogues constitute promising lead compounds as chemotherapy agents against several types of cancer.

1. Introduction

Colchicine is an alkaloid isolated from *Colchicum autumnale*. [1] It is used for the treatment of acute gout, familial Mediterranean fever, Behçet's disease, pericarditis, and other medical conditions.[2–12] It also acts as an anticancer agent and its mechanism of action is well-described in the scientific literature and is linked to its ability to inhibit mitosis. Specifically, colchicine binds to β-tubulin and forms complexes with tubulin dimers, which destabilizes microtubules and suppresses microtubule dynamics preventing mitotic spindle formation. This consequently leads to mitotic arrest and cell death typically *via* apoptosis.[13–16] Despite numerous pre-clinical findings highlighting beneficial effects of colchicine treatment for various types of cancers, its clinical application remains limited mainly to anti-inflammatory indications, due to its associated side-effects. To overcome those limitations, efforts are focused on developing more clinically-applicable colchicine derivatives.[17–40].

Brossi *et al.* synthesized a series of *N*-acyl and *N*-aroyl derivatives prepared from deacetylcolchicine. Several compounds showed high potency in the lymphocytic leukemia P388 screens *in vitro* and *in vivo*.[41] Later Kerekes *et al.* synthesized analogues of thiocolchicine, a very potent inhibitor of tubulin polymerization and cell growth, including *N*-

* Corresponding author.
E-mail address: adhucz@amu.edu.pl (A. Huczyński).

https://doi.org/10.1016/j.bmc.2021.116014
Received 1 July 2020; Received in revised form 30 December 2020; Accepted 4 January 2021
Available online 11 January 2021

acyldeacetylthiocolchicines, *N*-(alkoxycarbonyl)deacetylthiocolchicines, thiodemecolchicine and its methyl carbamate, as well as *O*-ethyl ethers of demethylthiocolchicines.[42] Both novel and previously described analogues were evaluated *in vitro* in a tubulin binding assay, *in vivo* in mice for acute toxicity, and in the P388 lymphocytic leukemia model.[42] Sun et al. subsequently reported three series of novel thiocolchicine analogs, *N*-acyl-, *N*-aroyl-, and *N*-(substituted benzyl)-deacetylthiocolchicinoids.[43] Those derivatives were evaluated for their cytotoxicity against various tumor cell lines, with particular emphasis on solid tumor cell lines, and for their inhibitory effects on tubulin polymerization *in vitro*. In 2011, Takayama's research group published results of their studies on C-4 halogen substituted colchicine derivatives, including 4-iodocolchicine.[29] 4-iodocolchicine showed *in vitro* similar potency against A549, HT29 and HCT116 cancerous cell lines to other halogenated colchicine derivatives in the C-4 position. Despite satisfactory results, to the best of our knowledge, it has not been implemented in *in vivo* studies or has not been further modified. In our previous research, we developed the concept of double-[33] and triple-modified colchicine analogs with diversified carbamate[34,35,44] or amide[45,46] substituents in the C-7 position. 4-iodothiocolchicine, double-modified colchicine derivative in the C-4 and C-10 position, showed very high potency against A549, MCF-7 and LoVo cancerous cell lines in the nanomolar range, higher than the activity of unmodified colchicine or 4-iodocolchicine. Interestingly, the high antiproliferative activity of 4-iodothiocolchicine was combined with beneficial selectivity index values.[33] Also the majority of novel triple-modified derivatives showed antiproliferative activity in the nanomolar range together with beneficial selectivity index values when tested against normal cells. Encouraged by the previously reported results, we sought to synthesize two series of novel double-modified derivatives of *N*-deacetylthiocolchicine and triple-modified derivatives of 4-iodo-*N*-deacetylthiocolchicine. In this study, we describe their synthesis, molecular docking, and anti-proliferative activities against several cancer cell lines.

2. Results and discussion

2.1. Chemistry

Compounds **2**–**3, 11**–**13** were obtained according to previously described procedures.[29,33,42] Double-modified (**4**–**10**) derivatives were synthesized in one pot reaction of compound **3** with respective acyl (**4**–**9**) or carbamoyl (**10**) chloride in the presence of triethylamine and 4-dimethylaminopyridine (DMAP) (see Scheme 1). Compound **6** was previously synthesized by Kerekes *et al.*[42] Triple-modified derivatives (**14**–**20**) were synthesized analogously starting with the compound **13** (see Scheme 1). The structures and purity of all products **2**–**20** were determined using the ESI-MS, FT-IR, ^{1}H NMR and ^{13}C NMR methods (see exemplary NMR spectra Fig. S1-S8).

2.2. In vitro cytotoxic activity evaluation

The seven double-modified derivatives (**4**–**10**), triple-modified colchicine derivatives (**14**–**20**), other colchicine derivatives (**2**–**3, 11**–**13**), and the starting material (**1**) were evaluated for their *in vitro* antiproliferative effect on acute lymphoblastic leukemia cells (ALL-5) and four human cancer cell lines: human lung adenocarcinoma (A549), human breast adenocarcinoma (MCF-7), human colon adenocarcinoma (LoVo) and its doxorubicin-resistant subline (LoVo/DX) as well as on normal murine embryonic fibroblasts (BALB/3T3). The data, expressed as $IC_{50} \pm SD$ of the tested compounds, are presented in Table 1[47,48] and the viability curves for ALL cells are shown in Supplemental Figure S9. Some general conclusions based on these data can be drawn. First, the majority of novel double-modified analogs of 7-deacetyl-10-thiocolchicine showed activity greater than or comparable to the unmodified colchicine towards primary ALL-5, A549, MCF-7 and LoVo cells (exception are compounds **9** and **10**). Although the compounds **4**–**8** have different substituents in the C-7 position, that does not seem to have a significant impact on these derivatives' activity, since the IC_{50} values against all the tested cancer cell lines are quite similar. The situation is different in case of triple-modified 4-iodo-7-deacetyl-10-thiocolchicine analogs. Compounds **14** and **17** showed the highest activity toward primary ALL-5, A549, MCF-7 and LoVo cells, and **16** showed moderate activity. The structural differences in the C-7 position have bigger impact on the IC_{50} values of triple-modified derivatives comparing to double-modified ones. Second, the greatest improvement in the activity of the new derivatives, in comparison to the colchicine, was observed for the A549, LoVo and LoVo/DX cell lines. The most active compounds were the following: against A549, **4**–**9**, **14**, **16**–**17** (approx. 9–12 fold more active than **1**); against LoVo, **4**– **9**, **14**, **16**–**18** (approx. 12–15 fold more active than **1**, compound **6** had even 19 times lower IC_{50}); against LoVo/DX, **4**–**9**, **14**, **16**–**18** (approx. 10–20 fold more active than **1**, compound **6** had even 30 times lower IC_{50}). For the primary acute lymphoblastic leukemia cells (ALL-5) and MCF-7 cells only the moderate improvement in the activity of the new derivatives was observed and the most active compounds were the following: against ALL-5, **5**–**8** (approx. 1,5 fold more active than **1**); and against MCF-7, **4**–**8**, **14**, **17** (approx. 1,5–2 fold more active than **1**). All of the above-listed compounds had very low, single- or double-nanomolar IC_{50} values, which are lower, than those presented for doxorubicin and cisplatin, currently widely

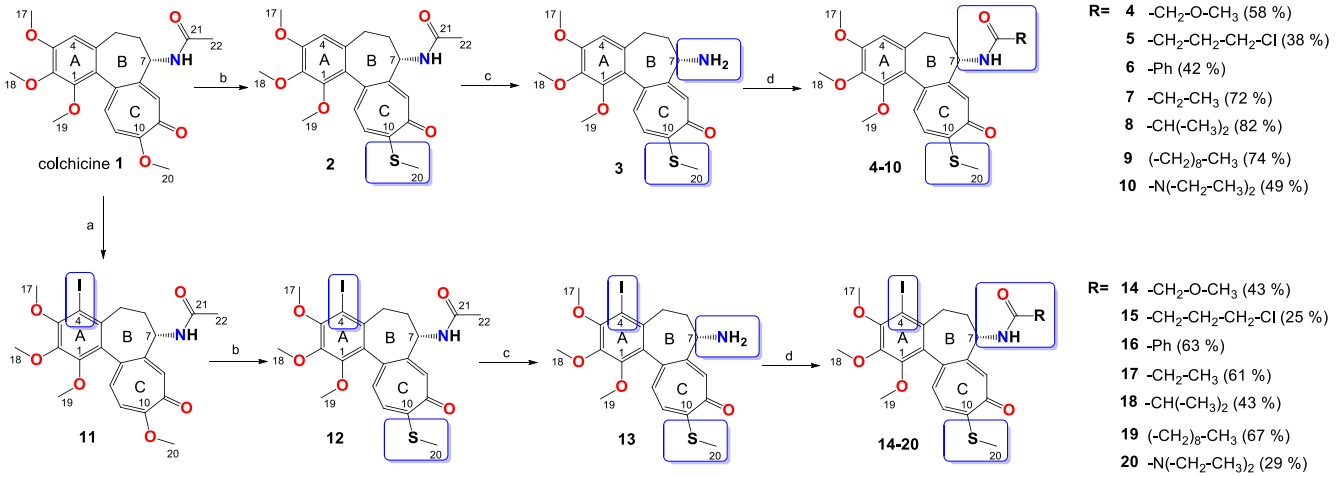

Scheme 1. Synthesis of colchicine derivatives (**2**–**20**). Reagents and conditions: (a) NIS, AcOH, 70 °C, 20 h (b) MeOH/H_2O, CH_3SNa, RT; (c) 2 M HCl, 90 °C, 72 h; (d) Et_3N, DMAP, respective acyl/carbamoyl chloride, THF, 0 °C → RT.

used as antitumor agents in cancer chemotherapy. Third, all of the tested derivatives were more active against LoVo cell line in comparison to its drug-resistant cell line LoVo/DX. Compounds **13** and **19** showed the weakest activity against all cancer cell lines tested (with the exception of **13** on LoVo/DX). When comparing double- (**4**–**10**) and triple-modified (**14**–**20**) derivatives, in many cases the derivatives with the same substituents in C-7 position showed similar IC_{50} values as for compounds **4** and **14** (except BALB/3T3 against which compound **14** turned out to be less potent), compounds **7** and **17**, and compounds **10** and **20** (except ALL-5 against which compound **20** turned out to be less potent). However, some differences between corresponding pairs should be highlighted. Compound **15** showed, depending on the cell line, 4–8 times higher IC_{50} in comparison to compound **5**. Compounds **6** and **16** showed similar IC_{50} against A549, LoVo and LoVo/DX cell lines, but compound **16** was 4–5 times less potent against ALL-5, MCF-5 and BALB/3T3 cell lines than **6**. Compounds **8** and **18** showed similar IC_{50} against LoVo and BALB/3T3, but compound **18** was about 4 times less potent against ALL-5, A549 and MCF-7 cell lines. Surprisingly, compound **18** was more active against LoVo/DX than **8**. The biggest difference can be observed between derivatives **9** and **19**; the derivative of *N*-deacetylthiocolchicine bearing long alkyl chain (**9**) proved to be much more active than the corresponding derivative of 4-iodo-*N*-deacetylthiocolchicine (**19**). These differences are further discussed in the molecular docking section in terms of binding affinities to the colchicine-binding pocket and structural differences between colchicine derivatives.

In our previous papers, analogues of 4-chloro-*N*-deacetylthiocolchicine[45] and 4-bromo- *N*-deacetylthiocolchicine[46] were described. The less potent derivatives in all 4-halo series were amides with long hydrophilic alkyl chains (like **19** from 4-iodo derivatives). Interestingly, the same substituent in the C-7 position did not decrease significantly the activity of double-modified derivative (**9**). The moderate potency, in all series, was also showed by ureas (like **10**, **20**), derivatives with 4-chlorobutanamide moiety in the C-7 position (like **5**, **15**), and for 4-iodo series also benzamide derivative (**16**). The highest activity, in all series, showed compounds bearing given moieties in the C-7 position: methoxyacetamide (like **4**, **14**), benzamide (like **6**, except 4-iodo derivative **16**), propionamide (like **7**, **17**) and isobutyramide (like **8**, **18**).

In order to evaluate the activity of the new analogs against cells with an MDR (multidrug resistance) phenotype, one drug resistant cancer cell line, LoVo/DX, was tested, and the resistance index (RI) values were calculated, as described in Materials and Methods and presented in Table 1. However, none of the derivatives was able to overcome the drug resistance of the LoVo/DX cell line, indicated by RI values ranging from 6.7 to 278.

Comparison of IC_{50} values between cancer cell lines and normal murine fibroblasts (BALB/3T3) was made to calculate the Selectivity Index (SI) as an initial indication of the compound's therapeutic potential (Fig. 1). Standard cancer chemotherapeutics utilized in this study (doxorubicin and cisplatin) are characterized by very low SI values < 1 (with the exception of doxorubicin on ALL-5, SI = 4.2 and on LoVo, SI = 1.8). The majority of double- and triple-modified analogues as well as their precursors showed favorable SI > 1.0 towards ALL-5 cells and A549, MCF-7 and LoVo cell lines. The exceptions are compounds: **4** on A549 and MCF-7; **10** on A549 and MCF-7; **13** on MCF-7; **19** on all cells studied. A beneficial SI on LoVo/DX cell line was observed only for compounds **3** and **13**. In general, the parent (unmodified) colchicine is characterized by higher SI values than doxorubicin and cisplatin (except doxorubicin on the LoVo cell line). Despite that, the following analogues showed higher SI values than parent colchicine: **2, 3, 8, 12** on ALL-**5**; **2**, **3**, **5**–**9**, **11**–**18**, **20** on A549; **2**, **3**, **12**, on MCF-7; **2**–**18**, **20** on LoVo; **2**, **3**, **5**, **6**, **8**, **9**, **12**–**16, 18** on LoVo/DX. This is important since high SI values result from large differences between the cytotoxicity against cancer versus normal cells, which might indicate that cancer cells will be affected to a greater extent than normal cells.

2.3. The effect of colchicine and its double- and triple-modified analogues on cell cycle progression in ALL-5 and MCF-7 cells

In order to further investigate the mechanism behind the favorable activity of colchicine (**1**) and its analogues towards primary ALL-5 cells, we assessed DNA content and DNA fragmentation *via* flow cytometry.

Table 1
Antiproliferative activity (IC_{50}) and resistance index (RI) values of colchicine (**1**) and its derivatives (**2**–**20**) compared with antiproliferative activity of standard anticancer drugs doxorubicin and cisplatin.[32–35]

Compound	ALL-5 IC_{50} (nM)	A549 IC_{50} (nM)	MCF-7 IC_{50} (nM)	LoVo IC_{50} (nM)	LoVo/DX IC_{50} (nM)	RI	BALB/3T3 IC_{50} (nM)
1	8.6 ± 0.2	125 ± 13	20.7 ± 2.4	108 ± 25	1,694 ± 275	*15.7*	106 ± 23
2	3.1 ± 1.3	11.3 ± 1.4	9.6 ± 2.4	21.0 ± 5.5	398 ± 75	*19.0*	137 ± 59
3	16.3 ± 4.9	24.1 ± 2.7	14.2 ± 1.6	16.9 ± 4.0	145 ± 21	*8.6*	223 ± 32
4	8.5 ± 0.2	13.5 ± 0.1	12.7 ± 1.3	8.2 ± 1.3	132 ± 44	*16.0*	12.0 ± 1.3
5	5.9 ± 0.1	13.3 ± 1.2	11.9 ± 1.2	8.4 ± 0.1	102 ± 15	*12.2*	20.2 ± 10.5
6	5.7 ± 1.9	11.2 ± 1.2	11.2 ± 1.2	5.6 ± 3.2	57.9 ± 13.5	*10.4*	21.6 ± 17.6
7	4.6 ± 0.6	13.2 ± 1.3	12.4 ± 1.3	8.5 ± 1.3	163 ± 51	*19.1*	17.9 ± 1.3
8	5.5 ± 0.1	15.8 ± 3.9	13.5 ± 0.02	9.0 ± 0.1	174 ± 46	*19.3*	69.9 ± 24.4
9	27.3 ± 0.5	13.3 ± 0.2	66.3 ± 25.5	7.6 ± 0.1	84.6 ± 1.1	*11.2*	87.2 ± 25.1
10	17.4 ± 5.1	133 ± 6	113 ± 7	69.1 ± 11.7	1,105 ± 191	*16.0*	88.2 ± 10.0
11	15.5 ± 1.6	93.9 ± 5.8	97.7 ± 29.3	10.2 ± 2.2	2,776 ± 449	*278.0*	135 ± 56
12	8.7 ± 0.2	11.1 ± 1.8	16.6 ± 6.4	7.4 ± 1.8	642 ± 84	*91.7*	115 ± 44
13	135 ± 35	866 ± 320	1,705 ± 361	126 ± 43	844 ± 52	*6.7*	1,424 ± 304
14	15.0 ± 5.9	10.5 ± 1.8	10.5 ± 1.8	7.0 ± 0.1	92.2 ± 19.3	*13.2*	51.2 ± 20.0
15	47.5 ± 9.0	82.8 ± 4.4	89.4 ± 6.6	39.2 ± 5.8	529 ± 77	*13.5*	87.8 ± 23.2
16	25.4 ± 0.8	13.3 ± 4.4	47.5 ± 14.9	7.2 ± 1.0	72.9 ± 5.0	*10.2*	76.2 ± 16.3
17	9.0 ± 1.1	11.4 ± 1.0	10.8 ± 1.8	7.2 ± 0.1	168 ± 66	*23.3*	39.6 ± 13.9
18	19.9 ± 5.2	62.6 ± 5.6	44.5 ± 23.6	7.0 ± 0.1	91.3 ± 16.8	*13.0*	69.7 ± 18.4
19	615 ± 181	833 ± 60	846 ± 117	568 ± 43	3,866 ± 1,328	*6.8*	305 ± 138
20	81.9 ± 16.5	81.3 ± 17.6	94.7 ± 7.5	64.6 ± 1.0	794 ± 134	*12.3*	107 ± 32
Doxorubicin	39.1 ± 7.0	258 ± 44	386 ± 118	92.0 ± 18.0	4,7500 ± 990	*51.6*	166 ± 74
Cisplatin	–*	6,367 ± 1,413	10,700 ± 753	4,370 ± 73	5,700 ± 630	*1.3*	3,900 ± 1,500

The IC_{50} value is defined as the concentration of a compound at which 50% growth inhibition is observed.
*Inhibition of proliferation did not exceed 50% at the highest concentration tested of 10 μM.
The RI indicates how many times a resistant subline is chemoresistant relative to its parental cell line. The RI was calculated for each compound using the formula: RI = IC_{50} for LoVoDX/IC_{50} for LoVo cell line. When RI is 0–2, the cells are sensitive to the compound tested, RI in the range 2–10 means that the cell shows moderate sensitivity to the drug tested, RI above 10 indicates strong drug-resistance.

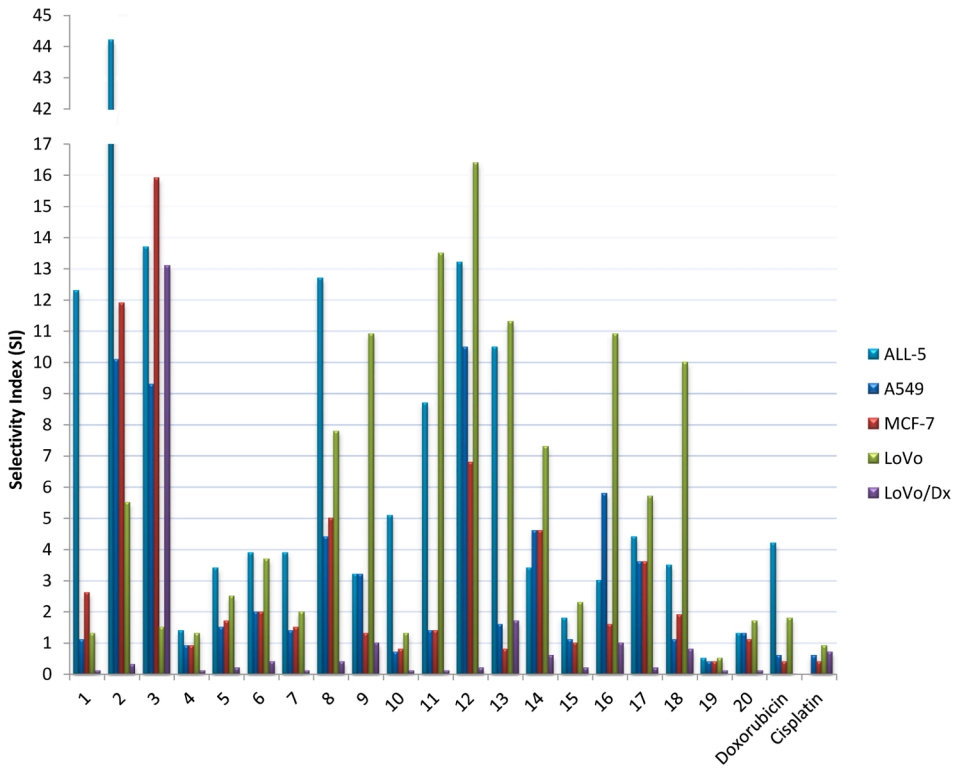

Fig. 1. Comparison of selectivity index (SI) values for the tested compounds. SI was calculated for each compound using the formula: SI = IC_{50} for normal cell line BALB/3T3/IC_{50} for respective cancerous cell line. A beneficial SI > 1.0 indicates a drug with efficacy against tumor cells greater than the toxicity against normal cells.

Specifically, propidium iodide staining was employed to determine DNA content and cells with sub-G1 (<2N) DNA were assessed as dead. Primary ALL-5 cells were treated for 24, 48 or 72 h with unmodified **1**, the most active synthesis precursors **2** and **12** (characterized by the lowest IC_{50} values, see Table 1) as well as double- and triple-modified analogues (**4**–**8** and **17**, respectively), each at concentrations equal to 5 × IC_{50} values. Treatment with 0.1% DMSO (vehicle) or 0.2 μM DX at equivalent time intervals served as negative and positive controls, respectively. For the full set of representative cytograms, see Supplemental Figure S10A. A graphical representation of cells in different phases of the cell cycle has been summarized from the mean of 3 experiments and presented in Fig. 2A. Statistically significant increases in sub-G1 DNA content were observed after 48 h of treatment with all of the compounds and further increased after 72 h (Fig. 2 A, orange bars). However, double-modified analogues **5**, **8** and synthesis precursor **12** induced DNA fragmentation more rapidly, as indicated by significant sub-G1 DNA after 24 h. The increase in sub-G1 DNA (Fig. 2A, orange bars) coincided with a decrease of the pool of cells in the G1 phase of the cell cycle (Fig. 2A, green bars), suggesting that in response to treatments ALL cells in G1 were susceptible to death. Since **1** is typically considered to induce cell death in the M phase,[49] it was of interest to investigate whether it, and the novel analogues, caused mitotic arrest in these cells. As shown in Fig. 2 A (red bars) the total amount of cells in the G2/M phases (4N DNA) was maintained at a relatively low level throughout, with a maximum of 20%, and no evidence of overt mitotic arrest was observed. Thus it appears that **1** and the analogues developed here induce death of primary ALL cells directly from the G1 not M phase, a finding consistent with previous results where we reported that two other microtubule destabilizing agents, vincristine and eribulin, exhibited this same property.[50] In contrast, when tested in MCF-7 cells, treatment with **1** and its analogues caused mitotic arrest, as indicated by accumulation of cells with 4N DNA (Fig. 2B, red bars; Supplemental Figure S10 B). Noteworthy also was the lack of significant sub-G1 DNA in treated MCF-7 cells, suggesting delayed death kinetics after arrest, or that they may die through a mechanism independent of DNA fragmentation, perhaps due to caspase-3 deficiency.[51]

2.4. The effect of colchicine, double-modified analogue 7 and triple-modified analogue 17 on PARP cleavage in primary ALL-5 cells

In order to further assess apoptotic cell death we investigated poly (ADP-ribose) polymerase (PARP) cleavage by immunoblotting. Primary ALL-5 cells were treated with parent colchicine (**1**) or the most active double- or triple-modified analogues (based on the lowest IC_{50} values, Table 1), namely compounds **7** and **17,** respectively, for 24 and 48 h. Treatment with 0.1% DMSO (vehicle) or 0.2 μM DX represented negative and positive controls, respectively. Representative immunoblots are shown in Fig. 3A and quantitation of PARP band intensities in Fig. 3B. All of the studied compounds induced loss of 116 kDa PARP over 48 h (Fig. 3 A, top panel and Fig. 3 B). The characteristic 85 kDa product of PARP degradation can be clearly observed for each treatment condition with **1** and its analogues. Treatment of ALL-5 cells with DX also induced PARP cleavage as we previously reported.[52,53] Glyceraldehyde 3-phosphate dehydrogenase (GAPDH) was used as a loading control (Fig. 3 A, lower panel).

2.5. Molecular docking

The primary mechanism of microtubule inhibitors involves binding to tubulin. Tubulin heterodimers composed of tightly bound α and ß tubulin monomers are the building blocks of microtubules, which are major components of the cytoskeleton of eukaryotic cells. Bundles of microtubules form mitotic spindles and hence are indispensable for cell division. Colchicine binds to β-tubulin, which results in microtubule destabilization since colchicine-bound dimers are assembly incompetent. Although most eukaryotic cells can express multiple isotypes of β tubulin, βI is typically the most highly expressed and most popular target for drug binding.[54] Molecular docking was applied to predict the

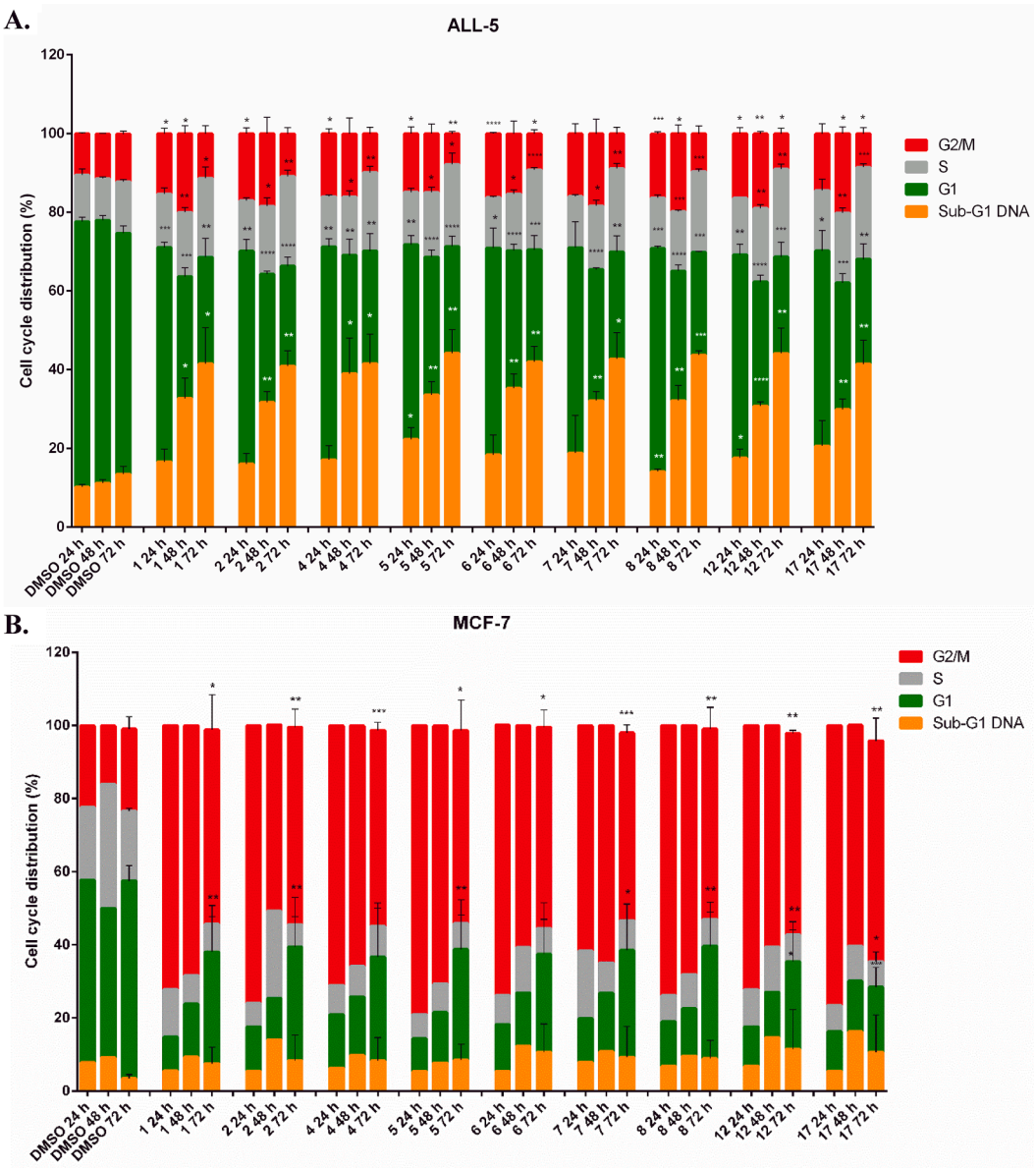

Fig. 2. ALL-5 (A) or MCF-7 (B) cells were treated with DMSO (vehicle), 1, or it's selected double- and triple-modified analogues for 24, 48 or 72 h and subjected to propidium iodide staining and flow cytometry. Percent of cells observed in different phases of cell cycle, determined by PI staining, is shown. Data are presented as a mean ± SD (n = 3 for all ALL-5 time points and MCF-7 at 72 h; for MCF-7 at 24 and 48 h, n = 1) ****P < 0.0001, ***P < 0.001, **P < 0.01, *P < 0.05 control versus dose. See Supplementa1 Fig. S9 for a full set of representative cytograms.

binding affinity of the new colchicine derivatives described in this paper with the colchicine-binding pocket of βI tubulin (Fig. 4, Table 2).[55]

Based on binding energies of the docking results, 13 out of 19 modification on colchicine, resulted in the lower binding energies compared to that of the unmodified colchicine, namely **2**–**9**, **12**, **14** and **16**–**18**. All the double-modified compounds except **10** and all the triple-modified ones except **15**, **19** and **20** show stronger interactions than colchicine alone. Based on the IC_{50} values obtained from cytotoxicity experiments, described in section 2.2, the most active synthetic precursors are **2**, **12**, **4**–**8**, **14** and **17**, respectively.

While in agreement with compounds **4** to **8** having the highest potency toward the investigated cell lines, the binding energies of compounds **5** to **7** show the lowest values but not in the same order. Compound **6** with −9.30 kcal/mol has the lowest binding energy and compounds **5** and **7** with values of −8.78 kcal/mol and −8.70 kcal/mol come after. Compounds **4** and **8** also have stronger binding energies, −8.30 and −8.25 kcal/mol, respectively compared with the unmodified colchicine, −8.09 kcal/mol.

Based on the *in silico* results, Compounds **17** and **14** with a triplet modification have the shared first and second position of the lowest binding energies of modified derivatives, −9.30 and −9.20 kcal/mol, respectively. As previously described, the above-mentioned compounds also show two of the highest potency with regards to the LoVo, LoVo/DX, A549 and MCF-7 cell lines.

Compounds **15**, **16** and **18** also show strong activity toward LoVo, LoVo/DX, A549 cell lines, although just compounds **16** and **18** were reported with the binding energy values lower than that for colchicine, i.e. −8.30 kcal/mol.

Consistently with the *in vitro* cytotoxic activity experiment results, compounds **13** and **19** have been found to have the highest binding energies, −6.90 and −7.05 kcal/mol.

None among the **2**, **3**, **11** and **12** compounds that show high potency toward different cell lines are amongst compounds with the lowest binding energies group. It is worth noting that except compound **11** that

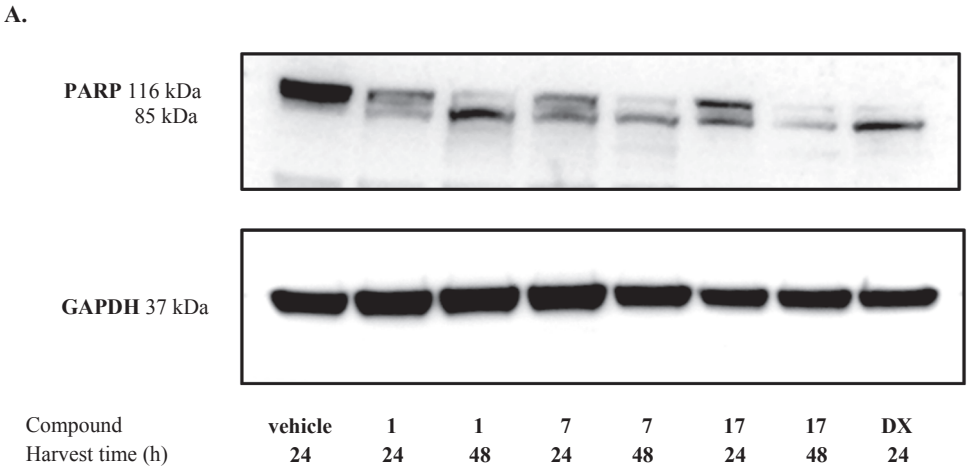

Fig. 3. (A) Cleavage of PARP. ALL-5 cells were treated with 43 nM compound **1**, 23 nM compound **7**, 45 nM compound **17**, 0.2 μM doxorubicin (**DX**), or 0.1% **DMSO** (vehicle) for the times indicated, and extracts were prepared and subjected to immunoblotting for PARP. The intact (116 kDa) and cleaved (85 kDa) forms of PARP are shown. GAPDH was used as a loading control. Images were quantified by measuring the band intensity using ImageJ software. (B) Bar diagram showing the fold changes of PARP normalized to GAPDH. Data represented as mean ± S.D. of three independent determinations (n = 3); 24 h treatment was compared with 48 h for respective compound. $^{**}P < 0.005$, $^{*}P < 0.05$.

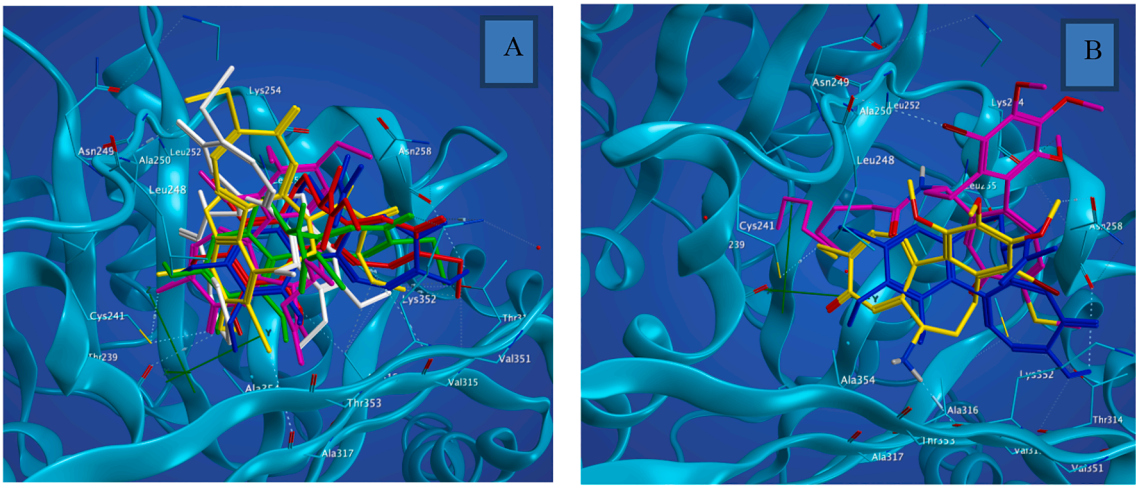

Fig. 4. A. The colchicine derivatives numbered **6, 17, 14, 5** and **7** show the strongest binding energies of −9.30, −9.30, −9.20, −8.78 and −8.70 kcal/mol, sequentially, unmodified colchicine added to the picture in white for comparison. B. compounds **13** and **19** have the highest binding energies, −6.90 and −7.05 kcal/mol, colchicine is added in blue.

has a higher binding energy than −8.09 the rest of the compounds still have stronger binding energies, −8.13, −8.25 and −8.13 kcal/mol respectively, than the binding energies of unmodified colchicine compounds.

To sum up, as predicted by our *in silico* calculations, we conclude that the colchicine derivatives numbered **6**, **17**, **14**, **5** and **7** show the strongest binding energies of −9.30, −9.30,

−9.20, −8.78 and −8.70 kcal/mol, respectively.

The two Met 259 and Lys 352 residues present in the binding pocket of βI tubulin are most strongly involved in the ligand-tubulin interactions. Met 259 and Lys 352 residues mostly interact with the hydrogen of C-20 (side chain H-acceptor) and oxygen of the carbonyl group (side chain H-donor) on ring C of the new colchicine derivatives, respectively. Previous research showed that substituting the *N*-acetyl group with an aliphatic, straight-chain acyl moiety group or an aromatic group on the acetamido group of the B ring might show some strong hydrophobic interactions with β tubulins. However, for example, adding hydrophilic ether function to the chain of the acetamido group can

Table 2
Summary of the calculated binding energies for the interactions between βI tubulin and *N*-deacetylthiocolchicine and 4-iodo-*N*-deacetylthiocolchicine analogues, the values of compounds' Moriguchi octanol-water partition coefficient (MlogP), which have been investigated in this paper. The active residues (residues interacting with each ligand *via* hydrogen bonding or π-interactions) in the binding pocket of βI tubulin are listed in the last column.

Compound	Binding energy (kcal/mol)	MlogP	Active residues
1	−8.09	1.368	Asn258, Met259
2	−8.13	2.127	Met259, Asn258, Lys352
3	−8.25	2.129	Asn258, Met259
4	−8.30	1.583	Ala 316, Lys352, Asn 258, Met 259
5	−8.78	2.761	Val 315, Met259, Lys254
6	−9.30	2.944	Val 315, Met259, Ala250
7	−8.70	2.342	Val 238, Met259, Lys352
8	−8.25	2.553	Cys 241, Ala316
9	−8.36	3.753	Val315
10	−7.40	2.813	Lys352, Met259, Asn258, Val238
11	−7.53	1.794	Ala317, Cys241
12	−8.13	2.553	Met259, Lys352
13	−6.90	2.570	Asn258, Cys241, Lys352
14	−9.20	2.001	Lys 352, Met259 Ala316, Ala317
15	−7.94	3.166	Lys 352, Met 259, Ala 250, Lys254, Cys241
16	−8.31	3.338	Asn258, Ala250, Lys254, Val238, Met259
17	−9.30	2.761	Lys 352, Met259, Ala316
18	−8.30	2.965	Cys241
19	−7.05	4.131	Lys254, Leu248
20	−7.63	3.219	Lys352, Asn258, Met259

decrease the compound's hydrophobicity.[20,56] Table 3 and Table S2 depict these interactions (see Table S1. for 2D-ligand-protein interactions representation).

In the 2D ligand-protein interactions scheme, see Table S1, greasy residues, which do not have a polar or charged sidechain, are shown in green. These residues are more likely to show hydrophobic interactions either with other protein residues or ligands. A proximity contour, shown as a dashed line, shows how deep a ligand is buried in the receptor cavity and if the ligand is surrounded by greasy residues, the most probable interactions between the ligand and greasy residues are hydrophobic reactions. The other parameter that plays a key role in the hydrophobic reactions is the ligand and receptor exposure, which shows the exposed part of a ligand or a residue to the water.

In the case of compound **6** and **16**, an aromatic functional group was substituted in the C-7 position that might induce the hydrophobic interactions between aromatic rings and greasy residues and result in a stronger interaction with βI tubulin. According to the *in vitro* cytotoxic activity experiments reported here, compound **6** has 5 and 4 times smaller IC_{50} values toward ALL-5 and LoVo cell lines than the IC_{50} values for compound **16**, respectively. Here, in the computational part, compound **6** also shows the lowest binding energy among the novel colchicine derivatives. It should be emphasized that while compound **16** has a binding energy which is higher than that for colchicine, the novel derivative is not in the group of top 5 compounds with the lowest binding energies. A side-by-side analysis of the 2D ligand-protein interactions schemes of compounds **6** and **16** shows that the aromatic group of compound **6** unlike that for compound **16**, is close to the proximity contour and deep in the receptor cavity, which might increase its hydrophobic interactions with hydrophobic side chains of the residues such as Ala 317, Leu248 and Leu252. For compound **16**, however, the blue circle around the aliphatic carbons represents the exposure of water to the functional group.

To investigate in more detail the non-bonded interactions of compound **6**, a contact preference map, electrostatic feature maps and the protein-ligand interaction fingerprints (PLIF) based on surface contact interactions were calculated (see figure S11). The data illustrate that Leu248 and Leu252 present hydrophobic interactions with an aromatic functional group in the C-7 position that might result in stronger binding energy with βI tubulin and a lower value of IC_{50} again for ALL-5 and LoVo cell lines.

Triple-modified compound **17** also has the highest binding energy and shares the first position in terms of the lowest binding energies for the modified derivatives. The binding energy of double-modified compound **7** also has the last position in the top 5 compounds with the lowest binding energies. Replacing the methyl group of acetamido group on carbon 7 on the B ring with ethyl group in compounds **7** and **17** improves the strength of their binding energies significantly. Based on the 3D ligand-protein interactions scheme, Table 3, the rings C and B of both compounds are in the same poses. Met259 has a sidechain H-acceptor with the hydrogen of carbon 20 on ring C and Lys352 has a sidechain H-donor with the oxygen of carbonyl on the same ring. The residues that interact with ring A of compound **17** and **7**, however, are different and this might be the reason for the 0.6 kcal/mol difference between their binding energies.

Compound **14** ranks in the second position among the compounds with the strongest interaction with βI tubulin. Adding hydrophilic ether groups to the chain of a functional group can decrease the hydrophobicity, so theoretically the binding energies of compound **4** and **14** should be lower than those for compound **7** and **17**. The binding energy of compound **4** is still lower than that for colchicine, but is not among the best modified compounds. To our surprise the binding energy for compound **14** is almost as good as those for compounds **6** and **17**. A possible explanation of this finding could be that the interaction between iodine atom on at carbon atom 4 of ring A and Ala 317 put the modified functional group of ring B in a position that can have a sidechain H-acceptors interacting with Lysine 352, a residue with an electrostatically-charged side chain, and Methionine 259. The above-mentioned interactions cause the added ether group to be less exposed to water and buried deeper into the cavity. It should be recalled that the

Table 3
Exemplary 3D representations of the interactions between βI tubulin, colchicine and its derivatives (**7** and **17**).

Compound	**1**	**7**	**17**
3D representation	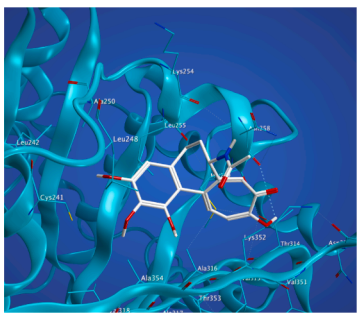	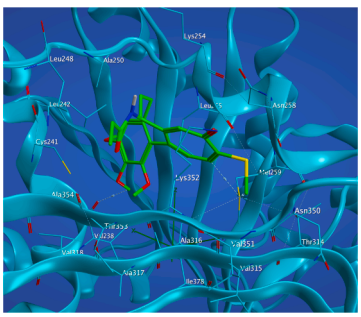	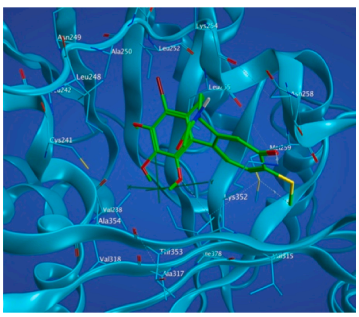

IC_{50} values for compounds **17** and **14** are almost the same for the MCF-7, A549 and LoVo cell lines.

Compound **5** is placed in the third position among the top 5 tubulin-binding compounds. Despite the fact that in both compounds **5** and **15**, methyl of acetamido group is replaced with 3-chloropropyl, the binding energies of double-modified, ligand **5**, and triple-modified, ligand **15**, are different as are their values of IC_{50} against all of the cell lines investigated here. Either in experimental or theoretical results, compound **5** shows to be a more desirable novel derivative than compound **15**. In a side-by-side comparison of the 2D interaction scheme for compound **5** and **15**, it can be found that sulfur of the Cysteine residue exhibits an interaction with sulfur of the substituted functional group on ring B for compound **5**. It is worth noting, that the interaction between sulfurs is not a disulfide bridge due to the fact that the two sulfurs are 3.68 Å apart which is longer than 2.05 Å of the disulfide bond length and hence can be categorized as a weak sulfur-sulfur interaction. Compound **15** has weaker binding energies than compound **5** even though it has a few hydrogen donors and acceptors interacting with residues, Lys352, Met259, Ala250, Lys 254 and Cys 241. The sidechain hydrogen acceptor interaction between Cys241 and hydrogen of carbon 7 in the 4-iodosubstitued compound is caused by inducing electronegativity on the ortho position of the subtitled iodine. This effect, puts the functional group of ring B in a position that is more exposed to water and hence engages in stronger hydrophilic interactions. The 3D molecular electrostatic potential map included in Table 4 shows a larger negative charge cloud over the oxygen of the ether group in the ortho position of iodine on the A ring. In compound **5**, the modified functional group is positioned in the receptor cavity and has less interface with water, which leads to a stronger interaction with the binding pocket of βI tubulin.

Consistently with experimental data, compound **13** and compound **19** are the weakest modified derivatives of colchicine that interact with βI tubulin. To investigate in detail the poor performance of compound **13**, 3D molecular electrostatic potential maps for compounds **3** and **13** were created for comparison. As is illustrated in Table 4, there is an enlarged negative charge cloud around the subtitled iodine on carbon 4 of ring A and the ether group in its ortho position. The intensified negative charge on ring A enhanced the hydrophilic interaction of ring A with water and resulted in weaker binding energies with βI tubulin.

A comparison of 2D and 3D interaction schemes between compound **9** and **19** in Table S1 and Table S2 shows that the only differences in their poses are the positions of their long hydrophobic aliphatic chains. The long functional group on ring B of compound **9** is surrounded by greasy residues and might result in an increased hydrophobic interaction, which might also explain higher cytotoxicity of compound **9** in comparison to compound **19**. It should be noted that long hydrophobic aliphatic chains can cause a steric effect which could jeopardize the cytotoxic activity of the novel derivatives, which is particularly confirmed by experimental data of compound **19**.

To provide a comparison between the computational and experimental results, linear regression coefficients were calculated. However, in numerous cases, the binding affinity alone is insufficient to arrive at a close correlation between the results of biological assays (and the values of IC_{50} given by them) and the binding free energies between the ligands and their protein targets obtained from docking computations. In order to account for the novel compounds' properties other than the affinity for the target, the Moriguchi octanol-water partition coefficients (MLogP) were calculated. MlogP is a useful factor to estimate and compare the distribution of drugs within biological systems such as the human body.

Thus, the two independent variables chosen in the compounds' characterization have been: MlogP values and the binding free energies with the tubulin βI isotype. Linear regression between IC_{50} values and these two variables was then performed and analyzed. A value of 0.5 is a good regression coefficient that has been found using this method for log IC_{50} of BALB/3T3 and LoVo cell lines. An acceptable value of 0.4 was obtained for LoVo/DX cell lines and the binding affinities for our compounds and tubulin βI isotype. The regression coefficient values obtained for the MCF-7, A549 and ALL-5 cell lines are very low. This may be due to off-target interactions, P-glycoprotein-based efflux of these compounds or additional complexities involved in the response of these cells to the compounds tested.

To take into account the fact that, regardless of their redundancy, all tubulin isotypes are expressed in a cell-based assay, the interaction energies involving the novel derivatives and the remaining isotypes of tubulin, namely: βIIa, βIIb, βIII, βIVa, βIVb, and βVI were calculated using the same docking method and comparisons of experimental data with computational results were made. It is worth noting that the ALL-5 cell line shows an acceptable linear regression coefficient 0.4 with βIIa and βVI isotypes (see Table 5). Low values of regression coefficients have

Table 5
The docking binding free energy values for the ligand-tubulin complexes and the MlogP predicted values for the ligands are two independent variables in the linear regression calculations with log IC_{50} [nM] for different cancer cell lines. The bolded value indicates the highest linear regression values.

Linear regression of colchicine derivatives (R^2)		ALL-5	MCF-7	LoVo	LoVo/DX	A549	BALB/3T3
	ßI	0.090	0.200	**0.500**	0.400	0.004	**0.500**
	ßIIa	0.400	0.100	0.040	0.100	0.040	0.001
	ßIIb	0.300	0.200	0.030	0.090	0.040	0.040
	ßIII	0.300	0.200	0.090	0.090	0.040	0.040
	ßIVa	0.20	0.300	0.200	0.020	0.200	0.200
	ßIVb	0.200	0.040	0.002	0.040	0.010	0.001
	ßV	0.200	0.100	0.110	0.020	0.040	0.002
	ßVI	0.400	0.100	0.060	0.002	0.090	0.010

Table 4
3D molecular electrostatic potential maps of compound **3** and **13** and **15**. The blue color represents negative charges and the red color represents positive charges.

Compound	3	13	15
3D-MEP map	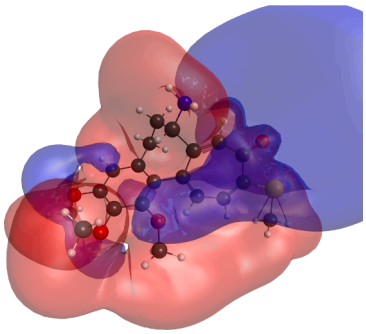	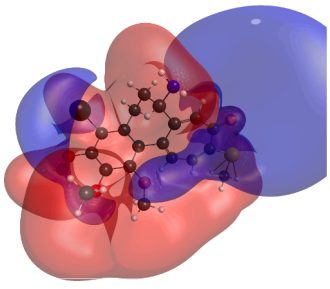	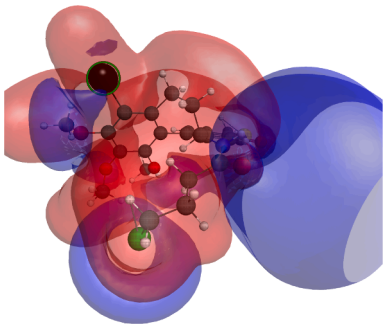

been found for the remaining tubulin isotypes. While these biological assays include millions of cells in a culture, computational work only focuses on a single protein at a time and its interaction with the pharmacological agent binding to it. Other biopharmaceutical properties should also be taken into account when theoretical and experimental results are compared. The upregulation of MDR proteins that act as efflux pumps for the tested compounds may be the main reason for some discrepancies between computation and experiment. Another possibility could involve off-target interactions whereby not only tubulin but also other proteins present in the tested cell lines bind these compounds lowering their measured potency.

3. Conclusions

We synthesized and characterized a set of 7-deacetyl-10-thiocolchicine and 4-iodo-7-deacetyl-10-thiocolchicine analogues. In total 19 colchicine derivatives, including 13 novel amide derivatives, were developed with moderate to good yields. Most of the derivatives showed activity against primary leukemia ALL-5 and established cancer cell lines (MCF-7, LoVo, LoVo/DX) in the low nanomolar range. In general, we conclude that 7-deacetyl-10-thiocolchicine analogues were more active towards ALL-5 cells while 4-iodo-7-deacetyl-10-thiocolchicine analogues were slightly more active towards the LoVo cell line. Most of the synthesized compound showed favorable selectivity index values, especially for ALL-5 and LoVo cell lines. Cell cycle progression studies revealed that colchicine and its derivatives induce death of primary ALL cells directly from G1 phase, as do other microtubule destabilizing agents such as vincristine and eribulin. In contrast, a lack of sub-G1 DNA after treatment of MCF-7 cells suggests delayed death kinetics after mitotic arrest. *In silico* calculations demonstrated that colchicine derivatives **6, 17, 14, 5** and **7** show the strongest binding energies of −9.30, −9.30, −9.20, 8.78 and −8.70 kcal/mol, respectively. These also exhibited very low nanomolar IC_{50} values in experimental assays. Favourable linear regression coefficients ($R^2 = 0.5$) were obtained for βI tubulin and LoVo as well as BALB/3T3 cell lines emphasizing the utility of molecular docking methodology for anticancer drug development.

4. Materials and methods

4.1. General

All precursors and solvents for the synthesis were obtained from Sigma Aldrich (Merck KGaA, Saint Louis, MO, USA) and were used without further purification. $CDCl_3$ spectral grade solvent was stored over 3 Å molecular sieves for several days. TLC was performed on precoated plates (TLC silica gel 60 F254, Aluminium Plates Merck, Merck KGaA, Saint Louis, MO, USA) visualized by illumination with an UV lamp. HPLC grade solvents (without further purification) were used for flash chromatography (CHROMASOLV from Sigma Aldrich, Merck KGaA, Saint Louis, MO, USA). The elemental analysis of compounds was performed on Vario ELIII (Elementar, Langenselbold, Germany).

4.2. Spectroscopic measurements

The ^1H, ^{13}C spectra were recorded on a Varian VNMR-S 400 MHz spectrometer (Varian, Inc., Palo Alto, CA, USA). ^1H NMR measurements of **2**–**20** (0.07 mol dm^{-3}) in $CDCl_3$ were carried out at the operating frequency 402.64 MHz. The error of the chemical shift value was 0.01 ppm. The ^{13}C NMR spectra were recorded at the operating frequency 101.25 MHz. The error of chemical shift value was 0.1 ppm. All spectra were locked to deuterium resonance of $CDCl_3$. The ^1H and ^{13}C NMR spectra are shown in the Supplementary Materials.

The FT-IR spectra of **2**–**20** in the mid infrared region were recorded in KBr. The spectra were taken with an IFS 113v FT-IR spectrophotometer (Bruker, Karlsruhe, Germany) equipped with a DTGS detector; resolution 2 cm^{-1}, NSS = 64. The Happ-Genzel apodization function was used.

The ESI (Electrospray Ionisation) mass spectra were recorded also on a Waters/Micromass (Waters Corporation, Manchester, UK) ZQ mass spectrometer equipped with a Harvard Apparatus syringe pump. The samples were prepared in dry acetonitrile (5 × 10–5 mol dm^{-3}). The sample was infused into the ESI source using a Harvard pump at a flow rate of 20 ml min^{-1}. The ESI source potentials were: capillary 3 kV, lens 0.5 kV, extractor 4 V. The standard ESI mass spectra were recorded at the cone voltages: 10 and 30 V. The source temperature was 120 °C and the desolvation temperature was 300 °C. Nitrogen was used as the nebulizing and desolvation gas at flow-rates of 100 dm^3 h^{-1}. Mass spectra were acquired in the positive ion detection mode with unit mass resolution at a step of 1 *m/z* unit. The mass range for ESI experiments was from *m/z* = 100 to *m/z* = 1000, as well as from *m/z* = 200 to *m/z* = 1500.

4.3. Synthesis

4.3.1. Synthesis of thiocolchicine (2)

To a mixture of **1** (500 mg, 1.25 mmol) in MeOH/water (1/1, *v/v*, 5 ml), the sodium methanethiolate (solution 21% in H_2O, 0.83 ml, 2.5 mmol) was added. The mixture was stirred in at RT for 72 h. Reaction time was determined by TLC. After that time, the reaction mixture was quenched by the addition of water (150 ml). The whole mixture was extracted four times with CH_2Cl_2, and the combined organic layers were dried over $MgSO_4$, filtered, and evaporated under reduced pressure. The residue was purified by CombiFlash® (hexane/EtOAc (1/1), then EtOAc/MeOH, increasing concentration gradient) to give **2** ($C_{22}H_{25}NO_5S$, MW = 415.5 g/mol) with yield 78% [57]. ^1H NMR (403 MHz, $CDCl_3$) δ 7.92 (s, 1H), 7.46 (s, 1H), 7.33 (d, J = 10.4 Hz, 1H), 7.10 (d, J = 10.5 Hz, 1H), 6.55 (s, 1H), 4.72–4.64 (m, 1H), 3.95 (s, 3H), 3.91 (s, 3H), 3.67 (s, 3H), 2.54 (dd, J = 13.0, 5.8 Hz, 1H), 2.45 (s, J = 5.7 Hz, 3H), 2.43–2.26 (m, 2H), 1.99 (s, 3H), 1.94 (dd, J = 11.8, 5.5 Hz, 1H) ppm. ^{13}C-NMR (101 MHz, $CDCl_3$) δ 182.4, 170.0, 158.1, 153.6, 151.8, 151.1, 141.6, 138.6, 134.8, 134.4, 128.3,126.7, 125.6, 107.3, 61.6, 61.4, 56.1, 52.3, 36.4, 29.9, 22.8, 15.1 ppm. FT-IR (KBr pellet): 3283, 2935, 1660, 1605, 1541, 1485, 1461, 1425, 1404, 1349, 1321, 1286, 1236, 1195, 1155, 1138, 1095, 1023 cm^{-1}. ESI-MS (*m/z*): $[M+H]^+$ calcd. 416, found 416, $[M+Na]^+$ calcd. 438, found 438, $[M+K]^+$ calcd. 454 found 454, $[2M+Na]^+$ calcd. 853, found 853, $[3M+Na]^+$ calcd. 1268, found 1268.

4.3.2. Synthesis of N-deacetylthiocolchicine (3)

Compound **3** was prepared from **2** by hydrolisys with 2 N HCl. To a solution of compound **2** (500 mg, 1.20 mmol) in MeOH (3 ml), the 2 N HCl solution (5 ml) was added. The mixture was stirred at 90 °C for 72 h. Reaction time was determined by TLC. After that time the reaction mixture was quenched by the addition of water (100 ml). The whole mixture was extracted four times with CH_2Cl_2, and the combined organic layers were dried over $MgSO_4$, filtered, and evaporated under reduced pressure. The residue was purified by CombiFlash® (EtOAc/MeOH, increasing concentration gradient) to give **3** ($C_{20}H_{23}NO_4S$, MW = 373.5 g/mol) with yield 86% [42]. ^1H NMR (403 MHz, $CDCl_3$) δ 7.58 (s, 1H), 7.19 (d, J = 10.3 Hz, 1H), 7.03 (d, J = 10.7 Hz, 1H), 6.54 (s, 1H), 3.91 (s, 3H), 3.91 (s, 3H), 3.75–3.69 (m, 1H), 3.66 (s, 3H), 2.52–2.26 (m, 6H), 1.65–1.57 (m, 3H) ppm. ^{13}C NMR (101 MHz, $CDCl_3$) δ 182.5, 157.8, 153.7, 153.4, 150.6, 141.1, 138.1, 135.2, 134.1, 129.3, 125.9, 125.4, 106.9, 61.1, 61.0, 56.0, 53.6, 40.2, 30.5, 15.1 ppm. FT-IR (KBr pellet): 3365, 3293, 2931, 2852, 2838, 1603, 1546, 1485, 1458, 1422, 1402, 1347, 1318, 1138, 1094, 1017 cm^{-1}. ESI-MS (*m/z*): $[M+H]^+$ calcd 374, found 374.

4.3.3. General procedure for the synthesis of colchicine derivatives (4–10)

Compounds **4**–**10** were obtained directly from compound **3**. To a solution of compound **4** (100 mg, 0.27 mmol) in tetrahydrofuran (THF, 5 ml) cooled to the 0 °C temperature, the following compounds were

added: Et_3N (2 ml, 14 mmol) and DMAP (catalytic amount). The mixture was first stirred at 0 °C temperature for a few minutes and then the solution of respective acyl chloride (**4**–**9**) or dietyhylcarbamoyl chloride (**10**) in THF (0.81 mmol in 2,5 ml) was added dropwise. The mixture was stirred at RT for the next 24 h. The solution was filtered to remove triethylamine hydrochloride. The THF was evaporated and the residue was purified by CombiFlash® (hexane/ethyl acetate, increasing concentration gradient) to give respective compounds as amorphous yellow solids with yield from 38% to 82% (**4**–**10**).

Compound **4**: ^{1}H NMR (403 MHz, $CDCl_3$) δ 7.26 (d, J = 10.3 Hz, 1H), 7.18 (s, 1H), 7.09 (d, J = 7.5 Hz, 1H), 7.02 (d, J = 10.6 Hz, 1H), 6.52 (s, 1H), 4.65 (dt, J = 11.8, 6.9 Hz, 1H), 3.92 (s, 3H), 3.88 (s, 3H), 3.83 (d, J = 4.3 Hz, 2H), 3.63 (s, 3H), 3.41 (s, 3H), 2.59–2.51 (m, 1H), 2.48–2.37 (m, 4H), 2.22 (tt, J = 13.0, 6.6 Hz, 1H), 1.88 (ddd, J = 11.9, 8.9, 5.8 Hz, 1H) ppm. ^{13}C NMR (101 MHz, $CDCl_3$) δ 182.3, 167.0, 158.2, 153.5, 151.2, 150.0, 141.6, 137.7, 134.4, 134.1, 128.5, 126.1, 125.6, 107.3, 71.6, 61.4, 61.3, 59.1, 56.0, 51.2, 36.8, 29.8, 15.1 ppm. FT-IR: 3287, 2937, 1672, 1607, 1552, 1486, 1462, 1426, 1403, 1350, 1323, 1287, 1264, 1236, 1195, 1154, 1138, 1096, 1022 cm^{-1}. ESI-MS (*m/z*): $[M+Na]^+$ calcd 468, found 468. Anal. Calcd. for C, 62.00; H, 6.11; N, 3.14; O, 21.55; S, 7.20; found C, 61.89; H, 6.05; N, 3.19; S, 7.35.

Compound **5**: ^{1}H NMR (403 MHz, $CDCl_3$) δ 7.55 (d, J = 7.4 Hz, 1H), 7.45 (s, 1H), 7.34–7.29 (m, 1H), 7.08 (d, J = 10.8 Hz, 1H), 6.53 (s, 1H), 4.70 (dt, J = 11.8, 6.9 Hz, 1H), 3.94 (s, 3H), 3.90 (s, 3H), 3.66 (s, 3H), 3.51 (td, J = 6.6, 1.1 Hz, 2H), 2.55–2.47 (m, 1H), 2.45–2.33 (m, 6H), 2.26 (dt, J = 18.6, 6.3 Hz, 1H), 2.08–1.99 (m, 2H), 1.94–1.86 (m, 1H) ppm. ^{13}C NMR (101 MHz, $CDCl_3$) δ 182.4, 171.5, 158.2, 153.6, 151.5, 151.1, 141.6, 138.4, 134.7, 134.3, 128.6, 126.6, 125.6, 107.3, 61.6, 61.4, 56.1, 51.9, 44.4, 36.8, 33.0, 30.0, 28.1, 15.12 ppm. FT-IR: 3273, 2937, 1669, 1604, 1531, 1486, 1461, 1428, 1403, 1368, 1346, 1320, 1282, 1234, 1194, 1156, 1138, 1092, 1020 cm^{-1}. ESI-MS (*m/z*): $[M+Na]^+$ calcd 500, found 500. Anal. Calcd. for C, 60.30; H, 5.90; Cl, 7.42; N, 2.93; O, 16.74; S, 6.71; found C, 60.46; H, 6.01; Cl, 7.44; N, 2.98; S, 6.69.

Compound **6**: ^{1}H NMR (403 MHz, $CDCl_3$) δ 7.83–7.79 (m, 2H), 7.68 (d, J = 7.3 Hz, 1H), 7.49 (s, 1H), 7.40–7.28 (m, 4H), 7.08 (d, J = 10.8 Hz, 1H), 6.56 (s, 1H), 4.91 (dt, J = 11.7, 6.8 Hz, 1H), 3.96 (s, 3H), 3.91 (s, 3H), 3.74 (s, 3H), 2.57 (dd, J = 13.3, 5.9 Hz, 1H), 2.50–2.40 (m, 4H), 2.35 (td, J = 12.4, 6.2 Hz, 1H), 2.07 (td, J = 11.7, 5.4 Hz, 1H) ppm. ^{13}C NMR (101 MHz, $CDCl_3$) δ 182.2, 166.8, 158.2, 153.6, 151.2, 141.6, 138.3, 134.6, 134.4, 133.5, 131.5, 128.7, 128.4, 127.1, 126.4, 125.7, 107.3, 61.7, 61.4, 56.1, 52.5, 36.6, 30.0, 15.1 ppm. FT-IR: 3334, 2937, 1658, 1605, 1545, 1528, 1485, 1461, 1424, 1404, 1350, 1322, 1287, 1235, 1195, 1154, 1137, 1095, 1020 cm^{-1}. ESI-MS (*m/z*): $[M+H]^+$ calcd 478, found 478, $[M+Na]^+$ calcd 500, found 500. Anal. Calcd. for C, 67.90; H, 5.70; N, 2.93; O, 16.75; S, 6.71; found C, 67.81; H, 5.78; N, 2.89; S, 6.79.

Compound **7**: ^{1}H NMR (403 MHz, $CDCl_3$) δ 7.39 (s, 1H), 7.30 (d, J = 10.3 Hz, 1H), 7.07 (d, J = 10.6 Hz, 1H), 6.52 (s, J = 4.6 Hz, 1H), 4.67 (dt, J = 11.8, 6.7 Hz, 1H), 3.93 (s, 3H), 3.89 (s, 3H), 3.66 (s, 3H), 2.51 (dd, J = 13.3, 6.2 Hz, 1H), 2.45–2.33 (m, 4H), 2.30–2.22 (m, 3H), 1.95–1.84 (m, 1H), 1.09 (t, J = 7.6 Hz, 3H) ppm. ^{13}C NMR (101 MHz, $CDCl_3$) δ 182.4, 173.6, 158.1, 153.5, 151.6, 151.1, 141.6, 138.4, 134.6, 134.4, 128.4, 126.6, 125.7, 107.3, 61.7, 61.3, 56.1, 51.9, 36.6, 29.9, 29.2, 15.1, 9.5 ppm. FT-IR: 3303, 2937, 1660, 1607, 1543, 1486, 1462, 1425, 1404, 1349, 1321, 1283, 1235, 1196, 1154, 1138, 1096, 1022 cm^{-1}. ESI-MS (*m/z*): $[M+H]^+$ calcd 430, found 430, $[M+Na]^+$ calcd 552, found 552 $[M+K]^+$ calcd 468, found 468. Anal. Calcd. for C, 64.31; H, 6.34; N, 3.26; O, 18.62; S, 7.42; found C, 64.41; H, 6.46; N, 3.22; S, 7.48.

Compound **8**: ^{1}H NMR (403 MHz, $CDCl_3$) δ 7.45 (s, 1H), 7.41 (d, J = 7.6 Hz, 1H), 7.32–7.28 (m, 1H), 7.06 (d, J = 10.8 Hz, 1H), 6.52 (s, 1H), 4.69 (dt, J = 11.8, 7.0 Hz, 1H), 3.93 (s, 3H), 3.89 (s, 3H), 3.67 (s, 3H), 2.51 (dt, J = 13.5, 6.8 Hz, 2H), 2.44–2.32 (m, 4H), 2.25 (dt, J = 18.6, 6.3 Hz, 1H), 1.89 (td, J = 11.8, 6.1 Hz, 1H), 1.12 (dd, J = 6.9, 4.0 Hz, 6H). ^{13}C NMR (101 MHz, $CDCl_3$) δ 182.3, 176.8, 158.0, 153.5, 151.7, 151.2, 141.6, 138.4, 134.5, 134.4, 128.6, 126.5, 125.7, 107.3, 61.7, 61.3, 56.1, 51.5, 36.7, 35.2, 30.0, 19.5, 19.5, 15.1 ppm. FT-IR: 3312, 2968, 2935, 1669, 1607, 1544, 1486, 1461, 1425, 1404, 1349, 1322, 1283, 1235, 1196, 1154, 1137, 1096, 1021 cm^{-1}. ESI-MS (*m/z*): $[M+Na]^+$ calcd 466, found 466. Anal. Calcd. for C, 64.99; H, 6.59; N, 3.16; O, 18.04; S, 7.23; found C, 64.87; H, 6.56; N, 3.15; S, 7.31.

Compound **9**: ^{1}H NMR (403 MHz, $CDCl_3$) δ 7.56 (d, J = 7.4 Hz, 1H), 7.45 (s, 1H), 7.31 (d, J = 10.4 Hz, 1H), 7.08 (d, J = 10.8 Hz, 1H), 6.54 (s, 1H), 4.71 (dt, J = 11.8, 6.9 Hz, 1H), 3.95 (s, 3H), 3.91 (s, 3H), 3.67 (s, 3H), 2.52 (dd, J = 13.3, 6.1 Hz, 1H), 2.46–2.34 (m, 4H), 2.30–2.21 (m, 3H), 1.89 (td, J = 11.9, 6.2 Hz, 1H), 1.58 (dd, J = 14.6, 7.2 Hz, 2H), 1.30–1.19 (m, 12H), 0.86 (t, J = 6.9 Hz, 3H) ppm. ^{13}C NMR (101 MHz, $CDCl_3$) δ 182.3, 173.0, 158.0, 153.5, 151.7, 151.1, 141.5, 138.4, 134.6, 134.4, 128.6, 126.5, 125.7, 107.3, 61.6, 61.3, 56.0, 51.8, 36.6, 36.3, 31.8, 30.0, 29.3, 29.3, 29.2, 29.2, 25.5, 22.6, 15.1, 14.0 ppm. FT-IR: 3298, 2927, 2853, 1655, 1607, 1543, 1485, 1461, 1425, 1404, 1348, 1321, 1282, 1235, 1195, 1154, 1137, 1097, 1022 cm^{-1}. ESI-MS (*m/z*): $[M+Na]^+$ calcd 550, found 550. Anal. Calcd. for C, 68.28; H, 7.83; N, 2.65; O, 15.16; S, 6.08; found C, 68.21; H, 7.98; N, 2.68; S, 5.98.

Compound **10**: ^{1}H NMR (403 MHz, $CDCl_3$) δ 7.48 (s, 1H), 7.26 (d, J = 10.4 Hz, 1H), 7.03–6.99 (d, J = 10.8 Hz, 1H), 6.50 (s, 1H), 5.90 (d, J = 7.1 Hz, 1H), 4.66 (dt, J = 11.7, 6.7 Hz, 1H), 3.91 (s, 3H), 3.87 (s, 3H), 3.67 (s, 3H), 3.32–3.25 (m, 4H), 2.48 (dd, J = 13.3, 5.7 Hz, 1H), 2.41–2.20 (m, 5H), 1.97–1.86 (m, 1H), 1.11 (t, J = 7.1 Hz, 6H) ppm. ^{13}C NMR (101 MHz, $CDCl_3$) δ 182.2, 157.8, 156.0, 153.3, 152.6, 151.1, 141.5, 138.4, 134.6, 134.3, 129.2, 126.2, 125.8, 107.2, 61.7, 61.3, 56.0, 53.1, 40.9, 37.2, 30.2, 15.0, 13.9 ppm. FT-IR: 3372, 2970, 2935, 1641, 1607, 1550, 1523, 1486, 1460, 1425, 1404, 1349, 1322, 1282, 1269, 1236, 1195, 1152, 1138, 1096, 1021 cm^{-1}. ESI-MS (*m/z*): $[M+H]^+$ calcd 473, found 473, $[M+Na]^+$ calcd 495, found 495, $[M+K]^+$ calcd 511, found 511. Anal. Calcd. for C, 63.54; H, 6.82; N, 5.93; O, 16.93; S, 6.78; found C, 63.41; H, 6.77; N, 6.01; S, 6.61.

4.3.4. Synthesis of 4-iodocolchicine (11)

A mixture of *N*-iodosuccinimide (560 mg, 2.49 mmol) and **1** (500 mg, 1.25 mmol) in AcOH was stirred at 70 °C under nitrogen atmosphere for the 20 h. Reaction time was determined by TLC. The reaction was quenched with saturated aqueous $Na_2S_2O_3$. The whole mixture was extracted four times with CH_2Cl_2, and the combined organic layers were dried over $MgSO_4$, filtered, and evaporated under reduced pressure. The residue was purified by CombiFlash® (EtOAc/MeOH, increasing concentration gradient) to give **11** with yield 95% [29]. ^{1}H NMR (403 MHz, $CDCl_3$) δ 8.22 (d, J = 5.6 Hz, 1H), 7.61 (s, 1H), 7.30 (d, J = 10.7 Hz, 1H), 6.89 (d, J = 11.2 Hz, 1H), 4.55–4.47 (m, 1H), 4.04 (s, 3H), 3.97 (s, 3H), 3.95 (s, 3H), 3.63 (s, 3H), 3.21–3.15 (m, 1H), 2.40 (dd, J = 12.7, 5.0 Hz, 1H), 1.99 (s, 3H), 1.87–1.81 (m, 1H) ppm. ^{13}C NMR (101 MHz, $CDCl_3$) δ 179.5, 170.2, 164.4, 153.4, 152.0, 151.4, 145.6, 136.7, 136.2, 135.6, 130.1, 129.5, 112.5, 92.1, 61.5, 61.3, 60.7, 56.5, 52.6, 34.4, 34.4, 22.7 ppm. FT-IR (KBr pellet): 3274, 2934, 1662, 1617, 1588, 1563, 1461, 1406, 1393, 1346, 1318, 1266, 1249, 1171, 1136, 1078, 1015 cm^{-1}. ESI-MS (*m/z*): $[M+H]^+$ calcd 526, found 526 $[M+Na]^+$ calcd 548, found 548.

4.3.5. Synthesis of 4-iodothiocolchicine (12)

To a mixture of **11** (500 mg, 0.95 mmol) in MeOH/water (1/1, v/v, 5 ml), the sodium methanethiolate (solution 21% in H_2O, 0.72 ml, 1.9 mmol) was added. The mixture was stirred in at RT for 72 h. Reaction time was determined by TLC. After that time the reaction mixture was quenched by the addition of water (150 ml). The whole mixture was extracted four times with CH_2Cl_2, and the combined organic layers were dried over $MgSO_4$, filtered, and evaporated under reduced pressure. The residue was purified by CombiFlash® (hexane/EtOAc (1/1), then EtOAc/MeOH, increasing concentration gradient) to give **12** ($C_{22}H_{24}INO_5S$, MW = 541.4 g/mol) as amorphous yellow solid with yield 71%.[33,57] ^{1}H NMR (403 MHz, $CDCl_3$) δ 7.75 (d, J = 6.9 Hz, 1H), 7.42 (s, 1H), 7.25 (d, J = 10.3 Hz, 1H), 7.09 (d, J = 10.8 Hz, 1H), 4.58–4.50 (m, 1H), 3.97 (s, 3H), 3.95 (s, 3H), 3.63 (s, 3H), 3.18 (dd, J =

13.7, 5.0 Hz, 1H), 2.46 (s, 3H), 2.40 (dd, J = 13.6, 6.2 Hz, 1H), 2.32–2.23 (m, 1H), 2.01 (s, 3H), 1.85–1.79 (m, 1H) ppm. ^{13}C NMR (101 MHz, $CDCl_3$) δ 182.4, 170.1, 159.1, 153.5, 151.4, 151.1, 145.6, 137.8, 136.8, 134.7, 129.7, 128.1, 126.3, 92.2, 61.6, 61.4, 60.8, 52.1, 34.5, 34.4, 22.9, 15.2 ppm. FT-IR (KBr pellet): 3288, 2936, 1660, 1607, 1547, 1461, 1406, 1346, 1318, 1288, 1262, 1197, 1138, 1081, 1019 cm^{-1}. ESI-MS (m/z): $[M+H]^+$ calcd 542, found 542, $[M+Na]^+$ calcd 564, found 564, $[M+K]^+$ calcd 580, found 580.

4.3.6. Synthesis of 4 -iododeacetylothiocolcicine (13)

Compound **13** was prepared from **12** by hydrolysis with 2 N HCl. To a solution of compound **12** (500 mg, 0.92 mmol) in MeOH (3 ml), the 2 N HCl solution (5 ml) was added. The mixture was stirred at 90 °C for 72 h. Reaction time was determined by TLC. After that time the reaction mixture was quenched by the addition of water (100 ml). The whole mixture was extracted four times with CH_2Cl_2, and the combined organic layers were dried over $MgSO_4$, filtered, and evaporated under reduced pressure. The residue was purified by CombiFlash® (EtOAc/MeOH, increasing concentration gradient) to give **13** ($C_{20}H_{22}INO_4S$, MW = 499.4 g/mol) with yield 83% [42]. ^{1}H NMR (403 MHz, cdcl$_3$) δ 7.59 (s, 1H), 7.11 (d, J = 10.3 Hz, 1H), 7.01 (d, J = 10.7 Hz, 1H), 3.93 (s, 6H), 3.62 (s, 3H), 3.57 (dd, J = 10.8, 6.2 Hz, 1H), 3.15–3.08 (m, 1H), 2.48–2.39 (m, 4H), 2.33–2.24 (m, 1H), 1.53–1.46 (m, 3H) ppm. ^{13}C NMR (101 MHz, cdcl$_3$) δ 182.5, 158.7, 153.4, 153.1, 150.9, 145.1, 137.7, 137.5, 133.8, 129.5, 129.2, 125.5, 91.7, 61.2, 61.0, 60.8, 53.4, 38.2, 35.1, 15.1 ppm. FT-IR (KBr pellet): 3375, 3309, 2932, 1605, 1553, 1460, 1405, 1343, 1313, 1246, 1195, 1136, 1081, 1014 cm^{-1}. ESI-MS (m/z): $[M+H]^+$ calcd 500, found 500. Anal. Calcd. for C, 48.10; H, 4.44; I, 25.41; N, 2.80; O, 12.82; S, 6.42; found C, 48.18; H, 4.54; I, 25.43; N, 2.75; S, 6.49.

4.3.7. General procedure for the synthesis of colchicine derivatives (14–20)

Compounds **14**–**20** were obtained directly from compound **13**. To a solution of compound **13** (100 mg, 0.20 mmol) in tetrahydrofuran (THF, 5 ml) cooled to the 0 °C temperature, the following compounds were added: Et_3N (2 ml, 14 mmol) and DMAP (catalytic amount). The mixture was first stirred at 0 °C temperature for a few minutes and then the solution of respective acyl chloride (**4**–**9**) or dietyhylcarbamoyl chloride (**10**) in THF (0.75 mmol in 2,5 ml) was added dropwise. The mixture was stirred at RT for the next 24 h. The solution was filtered to remove triethylamine hydrochloride. The THF was evaporated and the residue was purified by CombiFlash® (hexane/ethyl acetate, increasing concentration gradient) to give respective compounds as amorphous yellow solids with yield from 25% to 67% (**14–20**).

Compound **14**: ^{1}H NMR (403 MHz, $CDCl_3$) δ 7.20 (d, J = 7.6 Hz, 1H), 7.19 (s, 1H), 7.16 (d, J = 6.6 Hz, 1H), 7.03 (d, J = 10.6 Hz, 1H), 4.53 (dt, J = 11.8, 6.9 Hz, 1H), 3.97 (s, 3H), 3.94 (s, 3H), 3.87 (q, J = 15.0 Hz, 2H), 3.62 (s, 3H), 3.43 (s, 3H), 3.20 (dd, J = 13.9, 5.1 Hz, 1H), 2.52–2.42 (m, 4H), 2.28–2.17 (m, 1H), 1.80 (td, J = 12.0, 6.5 Hz, 1H) ppm. ^{13}C NMR (101 MHz, $CDCl_3$) δ 182.2, 169.2, 159.2, 153.4, 151.5, 149.4, 145.6, 137.0, 136.6, 134.3, 129.7, 128.3, 125.7, 92.1, 71.6, 61.4, 61.3, 60.7, 59.1, 51.1, 34.8, 34.4, 15.1 ppm. FT-IR: 3339, 2998, 2929, 1674, 1605, 1547, 1516, 1465, 1449, 1425, 1408, 1373, 1347, 1316, 1292, 1262, 1190, 1156, 1134, 1107, 1081, 1056, 1018 cm^{-1}. ESI-MS (m/z): $[M+Na]^+$ calcd 594, found 594. Anal. Calcd. for C, 48.34; H, 4.59; I, 22.21; N, 2.45; O, 16.80; S, 5.61; found C, 48.22; H, 4.51; I, 22.36; N, 2.46; S, 5.66.

Compound **15**: ^{1}H NMR (403 MHz, $CDCl_3$) δ 7.47 (d, J = 7.3 Hz, 1H), 7.42 (s, 1H), 7.23 (d, J = 10.4 Hz, 1H), 7.07 (d, J = 10.7 Hz, 1H), 4.57 (dt, J = 11.8, 6.9 Hz, 1H), 3.96 (s, 3H), 3.95 (s, 3H), 3.63 (s, 3H), 3.53 (t, J = 6.4 Hz, 2H), 3.16 (dd, J = 13.7, 5.0 Hz, 1H), 2.52–2.35 (m, 7H), 2.29–2.18 (m, 1H), 2.11–2.02 (m, 2H), 1.78 (td, J = 12.0, 5.6 Hz, 1H) ppm. ^{13}C NMR (101 MHz, $CDCl_3$) δ 182.3, 171.7, 159.2, 153.5, 151.4, 150.8, 145.6, 137.6, 136.7, 134.7, 129.6, 128.4, 126.2, 92.2, 61.6, 61.4, 60.8, 51.7, 44.4, 34.8, 34.5, 33.0, 28.1, 15.2 ppm. FT-IR: 3301, 2937, 1674, 1607, 1544, 1461, 1406, 1346, 1318, 1283, 1262, 1244, 1196, 1154, 1137, 1081, 1054, 1019 cm^{-1}. ESI-MS (m/z): $[M+Na]^+$ calcd 626, found 626. Anal. Calcd. for C, 47.73; H, 4.51; Cl, 5.87; I, 21.01; N, 2.32; O, 13.25; S, 5.31; found C, 47.74; H, 4.53; I, 20.89; N, 2.26; S, 5.27.

Compound **16**: ^{1}H NMR (403 MHz, $CDCl_3$) δ 7.93 (d, J = 7.1 Hz, 1H), 7.81 (dt, J = 8.5, 1.7 Hz, 2H), 7.52 (s, 1H), 7.37–7.32 (m, 1H), 7.29–7.23 (m, 3H), 7.10–7.05 (m, 1H), 4.79 (dt, J = 11.8, 6.9 Hz, 1H), 3.98 (s, 3H), 3.95 (s, 3H), 3.71 (s, 3H), 3.20 (dd, J = 13.7, 4.8 Hz, 1H), 2.52–2.42 (m, 4H), 2.31 (dt, J = 17.1, 4.9 Hz, 1H), 2.05 – 1.96 (m, 1H) ppm. ^{13}C NMR (101 MHz, $CDCl_3$) δ 182.2, 167.1, 159.2, 153.5, 151.5, 150.9, 145.6, 137.7, 136.9, 134.6, 133.3, 131.6, 129.8, 128.5, 128.4, 127.1, 126.1, 92.2, 61.7, 61.4, 60.8, 52.3, 34.7, 34.5, 15.2 ppm. FT-IR: 3323, 3058, 2935, 1659, 1606, 1549, 1487, 1461, 1406, 1346, 1319, 1289, 1262, 1197, 1152, 1081, 1019 cm^{-1}. ESI-MS (m/z): $[M+H]^+$ calcd 604, found 604, $[M+Na]^+$ calcd 626, found 626. Anal. Calcd. for C, 53.74; H, 4.34; I, 21.03; N, 2.32; O, 13.26; S, 5.31; found C, 53.79; H, 4.46; I, 20.97; N, 2.28; S, 5.33.

Compound **17**: ^{1}H NMR (403 MHz, $CDCl_3$) δ 7.53–7.48 (m, 1H), 7.40 (s, 1H), 7.24 (dd, J = 9.1, 4.0 Hz, 1H), 7.10—7.05 (m, 1H), 4.56 (dt, J = 11.9, 6.8 Hz, 1H), 3.97 (s, 3H), 3.95 (s, 3H), 3.64 (s, 3H), 3.17 (dd, J = 14.0, 4.6 Hz, 1H), 2.49–2.37 (m, 4H), 2.35–2.20 (m, 3H), 1.79 (td, J = 12.0, 5.2 Hz, 1H), 1.11 (dd, J = 9.8, 5.3 Hz, 3H) ppm. ^{13}C NMR (101 MHz, $CDCl_3$) δ 182.3, 173.8, 159.1, 153.4, 151.4, 151.0, 145.6, 137.7, 136.8, 134.6, 129.7, 128.2, 126.2, 92.2, 61.6, 61.4, 60.8, 51.7, 34.6, 34.5, 29.2, 15.2, 9.6 ppm. FT-IR: 3301, 2938, 1660, 1608, 1567, 1462, 1406, 1346, 1319, 1283, 1262, 1231, 1198, 1138, 1081, 1019 cm^{-1}. ESI-MS (m/z): $[M+H]^+$ calcd 556, found 556, $[M+Na]^+$ calcd 578, found 578. Anal. Calcd. for C, 50.62; H, 4.96; I, 22.29; N, 2.46; O, 14.05; S, 5.63; found C, 50.69; H, 4.91; I, 22.36; N, 2.41; S, 5.67.

Compound **18**: ^{1}H NMR (403 MHz, $CDCl_3$) δ 7.47 (d, J = 8.3 Hz, 2H), 7.23 (d, J = 10.3 Hz, 1H), 7.06 (d, J = 10.6 Hz, 1H), 4.58 (dt, J = 11.8, 7.0 Hz, 1H), 3.97 (s, 3H), 3.95 (s, 3H), 3.65 (s, 3H), 3.16 (dd, J = 13.8, 5.1 Hz, 1H), 2.55 (dt, J = 13.8, 6.9 Hz, 1H), 2.48–2.36 (m, 4H), 2.28–2.16 (m, 1H), 1.80 (td, J = 11.9, 5.3 Hz, 1H), 1.16 (dd, J = 6.9, 3.6 Hz, 6H) ppm. ^{13}C NMR (101 MHz, $CDCl_3$) δ 182.2, 177.0, 159.0, 153.4, 151.5, 151.1, 145.6, 137.7, 136.8, 134.5, 129.7, 128.5, 126.1, 92.2, 61.7, 61.3, 60.8, 51.3, 35.2, 34.7, 34.6, 19.5, 19.4, 15.1 ppm. FT-IR: 3331, 2970, 2935, 1669, 1608, 1552, 1461, 1406, 1345, 1319, 1284, 1262, 1239, 1198, 1153, 1137, 1081, 1019 cm^{-1}. ESI-MS (m/z): $[M+H]^+$ $[M+Na]^+$ calcd 592, found 592. Anal. Calcd. for C, 50.62; H, 4.96; I, 22.29; N, 2.46; O, 14.05; S, 5.63; found C, 50.71; H, 4.99; I, 22.31; N, 2.40; S, 5.59.

Compound **19**: ^{1}H NMR (403 MHz, $CDCl_3$) δ 7.40 (s, 1H), 7.23 (d, J = 10.3 Hz, 1H), 7.15 (d, J = 7.1 Hz, 1H), 7.06 (d, J = 10.8 Hz, 1H), 4.57 (dt, J = 11.9, 7.0 Hz, 1H), 3.97 (s, 3H), 3.95 (s, 3H), 3.63 (s, 3H), 3.17 (dd, J = 13.9, 5.0 Hz, 1H), 2.47–2.18 (m, 7H), 1.75 (td, J = 12.0, 5.2 Hz, 1H), 1.60 (td, J = 14.8, 7.3 Hz, 2H), 1.35–1.20 (m, 12H), 0.86 (t, J = 7.2 Hz, 3H) ppm. ^{13}C NMR (101 MHz, $CDCl_3$) δ 182.3, 173.2, 159.1, 153.4, 151.5, 150.9, 145.6, 137.6, 136.7, 134.5, 129.7, 128.3, 126.2, 92.2, 61.6, 61.3, 60.8, 51.6, 36.4, 34.8, 34.5, 31.8, 29.4, 29.3, 29.3, 29.2, 25.5, 22.6, 15.1, 14.1 ppm. FT-IR: 3298, 2927, 2856, 1656, 1607, 1547, 1461, 1406, 1346, 1319, 1283, 1262, 1246, 1198, 1154, 1138, 1081, 1019 cm^{-1}. ESI-MS (m/z): $[M+H]^+$ calcd 654, found 654. Anal. Calcd. for C, 55.13; H, 6.17; I, 19.42; N, 2.14; O, 12.24; S, 4.91; found C, 55.02; H, 6.19; I, 19.44; N, 2.19; S, 4.86.

Compound **20**: ^{1}H NMR (403 MHz, $CDCl_3$) δ 7.48 (s, 1H), 7.21–7.17 (m, 1H), 7.03–6.99 (m, 1H), 5.89–5.85 (m, 1H), 4.53 (dt, J = 11.7, 6.7 Hz, 1H), 3.94 (s, 3H), 3.92 (s, 3H), 3.64 (s, 3H), 3.30 (q, J = 7.1 Hz, 4H), 3.12 (dd, J = 13.8, 4.7 Hz, 1H), 2.44–2.33 (m, 4H), 2.28–2.18 (m, 1H), 1.81 (td, J = 12.0, 5.3 Hz, 1H), 1.12 (t, J = 7.1 Hz, 6H) ppm. ^{13}C NMR (101 MHz, $CDCl_3$) δ 182.2, 158.8, 156.0, 153.2, 152.1, 151.4, 145.5, 137.6, 137.0, 134.3, 129.9, 128.9, 125.9, 92.1, 61.7, 61.3, 60.7, 52.9, 41.0, 35.2, 34.8, 15.1, 13.9 ppm. FT-IR: 3383, 2973, 2935, 1639, 1608, 1553, 1525, 1492, 1460, 1425, 1406, 1344, 1318, 1284, 1264, 1216, 1183, 1152, 1137, 1080, 1018 cm^{-1}. ESI-MS (m/z): $[M+H]^+$ calcd 599, found 599, $[M+Na]^+$ calcd 621, found 621. Anal. Calcd. for C, 50.17; H, 5.22; I, 21.20; N, 4.68; O, 13.37; S, 5.36; found C, 50.08; H, 5.19; I,

21.21; N, 4.70; S, 5.41.

4.4. Cell lines and culturing conditions

Primary ALL-5 cells were derived from the bone marrow of a 37-year old patient as previously described.[58,59] Although these cells can be cultured up to 6 months with no obvious change in their properties,[58] in the present study they were exclusively used at low passage for all experiments, and are thus referred to as primary cells. Primary ALL-5 cells were routinely maintained at 37 °C in a humidified 5% CO_2 incubator in IMDM Modified (SH30228, HyClone) media supplemented with 10 μg mL^{-1} cholesterol (C3045, Sigma-Aldrich), 6 mg mL^{-1} human serum albumin (HA1000, Golden West Biologicals), 2 mM L-glutamine (25–005, Corning), 2% v/v amphotericin-B/penicillin/streptomycin (A2942, Sigma-Aldrich, 30–002, Corning), 1 μg mL^{-1} insulin (128–100, Cell Applications), 200 μg mL^{-1} apo-transferrin (T1147, Sigma-Aldrich), and 50 μM β-mercaptoethanol, and were subcultured to maintain a density of 1–3 × 10^6 cells mL^{-1}. Human MCF-7 mammary gland adenocarcinoma cells originally isolated from a 69 year old Caucasian woman with several characteristics of differentiated mammary epithelium were cultured in Eagle's Minimum Essential Medium (EMEM) (30-2003, ATCC, USA) supplemented with 10% (v/v) heat-inactivated fetal bovine serum (FBS) (FP-0500-A, Atlas Biologicals, USA), and 1% Penicillin/Streptomycin Solution 100x (30-002-Cl, Corning, USA). MCF-7 cell line was tested via short tandem repeat profiling in July 2018 by Genetica DNA Laboratories (Burlington, NC) and verified as authentic, giving a 100% match when compared to the known reference profile.[60] Both primary ALL-5 cells and MCF-7 cell line for cell cycle analysis were maintained in the Department of Biochemistry & Molecular Biology at University of Arkansas for Medical Sciences, USA.

The BALB/3T3 cell line was purchased from the American Type Culture Collection (ATCC Manassas, VA, USA), A549 and MCF-7 cell lines – from European Collection of Authenticated Cell Cultures (Salisbury, UK), LoVo cell line was purchased from the American Type Culture Collection (ATCC, Manassas, VA, USA), and LoVo/DX received courtesy of Prof. E. Borowski (Technical University of Gdańsk, Gdańsk, Poland). All of the above-listed cell lines were maintained in the Institute of Immunology and Experimental Therapy (IIET), Wroclaw, Poland. Human lung adenocarcinoma cell line (A549) was cultured in the mixture of OptiMEM and RPMI 1640 (1:1) medium (IIET, Wroclaw, Poland), supplemented with 5% fetal bovine serum (GE Healthcare, Logan UT, USA) and 2 mM L-glutamine (Sigma-Aldrich, Merck KGaA, Saint Louis, MO, USA). Human colon adenocarcinoma cell lines (LoVo) were cultured in mixture of OptiMEM and RPMI 1640 (1:1) medium (IIET, Wroclaw, Poland), supplemented with 5% fetal bovine serum (GE Healthcare, Logan, UT, USA), 2 mM L-glutamine, 1 mM sodium pyruvate (Sigma-Aldrich, Merck KGaA, Saint Louis, MO, USA) and 10 μg/100 ml doxorubicin for LoVo/DX (Sigma-Aldrich, Merck KGaA, Saint Louis, MO, USA). Murine embryonic fibroblast cells (BALB/3T3) were cultured in Dulbecco medium (Life Technologies Limited, Paisley, UK), supplemented with 10% fetal bovine serum (GE Healthcare, Logan, UT, USA) and 2 mM glutamine (Sigma-Aldrich, Merck KGaA, Saint Louis, MO, USA). All cell culture media contained antibiotics: 100 U/ml penicillin and 100 μg/ml streptomycin (Polfa-Tarchomin, Warsaw, Poland). All cell lines were cultured during entire experiment in humid atmosphere at 37 °C and 5% CO_2. Cells were tested for mycoplasma contamination by mycoplasma detection kit for conventional PCR: Venor *GeM* Classic (Minerva Biolabs GmbH, Berlin, Germany) and negative results were obtained. The procedure is repeated every year or in the case of less frequently used lines after thawing.

4.5. Cell viability assays

4.5.1. SRB assay

Sulforhodamine B (SRB) assay was performed to asses about cytotoxic activity of studied compounds towards adherent cell lines. Cells (10^4 per well) were seeded in 96-well plates (Sarstedt, Nümbrecht, Germany) in appropriate complete cell culture media and after 24 h prior addition of tested compounds. Cells were subjected to the treatment with tested agents or cisplatin (Teva Pharmaceuticals Polska, Warsaw, Poland) or doxorubicin (Accord Healthcare Limited, Middlesex, UK) in the concentration range 100–0.01 μg/ml for 72 h. Treatment with DMSO (POCh, Gliwice, Poland) at concentrations corresponding to these present in tested agents' dilutions was applied as a control (100% cell viability). After 72 h of incubation with the tested compounds, cells were fixed in situ by gently adding of 50 μL per well of cold 50% trichloroacetic acid TCA (POCh, Gliwice, Poland) following incubation at 4 °C for one hour.[47] Next, wells were washed four times with water and air dried. 50 μL of 0.1% solution of sulforhodamine B (Sigma–Aldrich, Merck KGaA, Saint Louis, MO, USA) in 1% acetic acid (POCh, Gliwice, Poland) were added to each well and plates were incubated at room temperature for 0.5 h. Unbounded dye was removed by washing plates four times with 1% acetic acid. Stained cells were solubilized with 10 mM Tris base (Sigma–Aldrich, Merck KGaA, Saint Louis, MO, USA). Absorbance of each solution was read at Synergy H4 Hybrid Multi-Mode Microplate Reader (BioTek Instruments, Inc., Winooski VT, USA) at the 540 nm wavelength.

Results are presented as mean IC_{50} (concentration of the tested compound, that inhibits cell proliferation by 50%) ± standard deviation. IC_{50} values were calculated in Cheburator 0.4, Dmitry Nevozhay software (version 1.2.0 software by Dmitry Nevozhay, 2004–2014, http://www.cheburator.nevozhay.com, freely available) for each experiment.[48] Compounds at each concentration were tested in triplicate in individual experiment and each experiment was repeated at least three times independently.

4.5.2. MTT assay

A 3-(4,5-dimethylthiazol-2-yl)-2,5-dimethylthiazol-2-yl)-2,5-diphenyltetrazolium bromide (MTT)-based assay,[61] was used to evaluate the effect of drugs on the viability of primary ALL-5 cells. Cells (10^5/well) in 100 μL of complete IMDM Modified medium were seeded in 96-well plates (TPP, Switzerland) and treated with drugs at concentrations up to 10 μM for 120 h with control cells receiving vehicle (0.1% DMSO) alone. After treatment, 10 μL of MTT solution (5 mg/mL) was added to each well, and the plate was incubated at 37 °C for 24 h in a humidified 5% CO_2 incubator. Then 100 μL of 10% SDS in 0.01 M HCl was added to each well and the plate was incubated at 37 °C for a further 24 h. The experiment was performed in quadruplate (n = 4). Absorbance was recorded at 540 nm using a BioTek Plate Reader. Inhibition of formation of colored MTT formazan was taken as an index of cytotoxicity activity. IC_{50} values were determined by non-linear regression analysis using GraphPad Prism 6 for Windows (GraphPad Software).

Selectivity index (SI) was calculated by dividing the IC_{50} value for BALB/3T3 cells by the IC_{50} value for individual cancer cell lines, and resistance index (RI) was calculated by dividing the IC_{50} for LoVo/DX cells by the IC_{50} for LoVo cells. The Resistance Index (RI) was defined as the ratio of IC_{50} for a given compound calculated for resistant cell line to that measured for its parental drug sensitive cell line (Table 1).

4.6. DNA content analysis

ALL-5 (1.5 × 10^6) and MCF-7 (0.2 × cells 10^6) were seeded in 100 mm Petri dishes (Corning, NY) and incubated in the presence of vehicle (0.1% DMSO) or compounds, at concentrations specified in the text, for 24, 48 or 72 h at 37 °C in a humidified 5% CO_2 incubator. Cells were then washed with 1 ml phosphate-buffer saline (PBS), fixed with 1–3 ml of 70% ice-cold ethanol and stored at 4 °C prior to flow cytometric analysis. Cells were centrifuged, treated with 500 μL propidium iodide/RNase Staining buffer (BD Biosciences, San Jose, CA, USA) and stored in the dark for 1 h at RT. The stained cells were subjected to a FacsAria IIIu Flow Cytometer (BD Biosciences, San Jose, CA, USA) performed by

UAMS Flow Cytomery Core Facility and data were analyzed using FlowJo software.

4.7. Western blot analysis

ALL-5 cells (15×10^6 cells/dish) were treated for 24 and 48 h with **1** and **5** at $5 \times IC_{50}$ values concentration or with vehicle (0.1% DMSO) or DX (0.2 μM) for 24 h. Cells were washed in PBS and lysed in lysis buffer (25 mM HEPES, pH 7.5, 300 mM NaCl, 0.1% Triton X-100, 1.5 mM $MgCl_2$, 0.2 mM EDTA, 0.5 mM DTT, EDTA-free complete protease inhibitor tablets (Roche), 20 μg ml^{-1} aprotinin, 50 μg ml^{-1} leupeptin, 10 μM pepstatin, 1 mM phenylmethylsulfonyl fluoride, 20 mM β-glycerophosphate, 1 mM Na_3VO_4, and 1 μM okadaic acid. Protein content was measured by Bradford assay and equal amounts (20 μg) were separated by electrophoresis using Mini-PROTEAN® precast gels (Bio-Rad). Proteins were electrophoretically transferred onto a PVDF membrane (Immobilon-FL, Merck Millipore) and next stained with Ponceau S to assess transfer efficiency and verify equal loading. The membrane was blocked with 5% nonfat milk in Tris-buffered saline containing 0.1% TWEEN-20 (TBS-T) for 1 h at RT and incubated overnight at 4 °C with primary antibodies (Santa Cruz Biotechnology) against PARP (9532) (1:2500 dilution) and GAPDH (2118) (1:10000 dilution). After washing with TBS-T for 5×5 min the membrane was incubated with secondary HRP-conjugated goat anti-rabbit IgG (H+L) antibody (1:5000 dilution) (Bio-Rad) for 1 h at RT. After washing in TBS-T the membrane was exposed to ClarityTM Western ECL Substrate luminol enhancer solution and peroxide solution (Bio-Rad) for 5 min and visualized and quantified using Image J software.

4.8. Statistical analysis

Unpaired *t* test with Welch's correction was performed for the significance and p values of <0.05 were considered significant.

4.9. Docking simulations

Docking of the *N*-deacetylthiocolchicine and 4-iodo-*N*-deacetylthiocolchicine derivatives was performed using AutoDock 4 software package. AutoDock4 includes AutoGrid calculation that pre-calculate atomic affinity potentials in the ligand docked binding site and predict poses for ligand with up to 10 flexible bonds with combination of grid values, the Lamarckian Genetic Algorithm and empirical free energy scoring function.[62] For our docking simulations, a cubic box with size $44.0 \times 44.0 \times 60.0$ $Å^3$ centered at the center of mass of the bound colchicine was considered. All cofactors, namely, GTP, GDP, colchicine, and the magnesium ion were removed during docking. The protein was kept rigid but the compounds were chosen to be flexible. The ligand structures were first energy-minimized, then fully optimized based on the RHF/cc-pVDZ level of theory implemented in the software package GAMESS-US, version 2010-10-01. Since there is no crystal structure for human βI tubulin (UniProt ID: P07437) available in the Protein Data Bank (PDB), the bovine tubulin structure 1SA0.pdb was used as a template to construct a homology model for human βI tubulin using the software package MOE2015. Note that this particular structure is appropriate for colchicine-derivative binding because it corresponds to a co-crystallized complex of tubulin with colchicine. Other β tubulin isotypes used for computational studies were: βIIa (UniProt ID: Q13885), βIIb (UniProt ID: Q9BVA1), βIII (UniProt ID: Q13509), βIVa (UniProt ID: P04350), βIVb (UniProt ID: P68371), and βVI (UniProt ID: Q9H4B7).

For every compound, docking was run separately on each of the tubulin representative structures obtained from clustering. The ligand poses were eventually rescored using AutoDock's scoring function. For every derivative, the pose with the best AutoDock score over all representative structures of each tubulin isotype was kept for further analysis, especially to investigate the correlation with experimental pIC50 values. Besides AutoDock scores, the Moriguchi octanol-water partition coefficient (MLogP) of every compound was calculated using the ADMET Predictor 8.0 package (ADMET Predictor, Simulations Plus, Lancaster, CA, USA). Both Vina scores and MlogP values were used as inputs to build a two-variable linear regression model for every tubulin isotype.

Declaration of Competing Interest

The authors declare that they have no known competing financial interests or personal relationships that could have appeared to influence the work reported in this paper.

Acknowledgments

Financial support by grant of the Polish National Science Centre (NCN) – No. 2016/21/B/ST5/00111 is gratefully acknowledged. GK gratefully acknowledges the doctoral scholarship "ETIUDA" – No. 2018/28/T/ST5/00041 financed by the Polish National Science Centre (NCN). T.C.C. acknowledges support from Arkansas Breast Cancer Research Program. The authors thank Ms. Andrea Harris from UAMS Flow Cytometry Core. JAT acknowledges funding support from NSERC (Canada), the Alberta Cancer Foundation and the Allard Foundation.

Appendix A. Supplementary data

Supplementary data to this article can be found online at https://doi.org/10.1016/j.bmc.2021.116014.

References

1 Wallace SL. Colchicine. *Semin Arthritis Rheum*. 1974;3:369–381. https://doi.org/10.1016/0049-0172(74)90006-7.
2 Shchegravina ES, Knyazev DI, Beletskaya IP, Svirshchevskaya EV, Schmalz HG, Fedorov AY. Synthesis of nonracemic pyrrolo-allocolchicinoids exhibiting potent cytotoxic activity. *Eur J Org Chem*. 2016;2016:5620–5623. https://doi.org/10.1002/ejoc.201601069.
3 Zemer D, Livneh A, Danon YL, Pras M, Sohar E. Long-term colchicine treatment in children with familial Mediterranean fever. *Arthritis Rheum*. 1991;34:973–977. https://doi.org/10.1002/art.1780340806.
4 Ben-Chetrit E, Levy M. Colchicine prophylaxis in familial Mediterranean fever: reappraisal after 15 years. *Semin Arthritis Rheum*. 1991;20:241–246. https://doi.org/10.1016/0049-0172(91)90019-V.
5 Cerquaglia C, Diaco M, Nucera G, La Regina M, Montalto M, Manna R. Pharmacological and clinical basis of treatment of Familial Mediterranean Fever (FMF) with colchicine or analogues: an update. *Curr Drug Targets Inflamm Allergy*. 2005;4:117–124. https://doi.org/10.2174/1568010053622984.
6 Masuda K, Nakajima A, Urayama A, Nakae K, Kogure M, Inaba G. Double-masked trial of cyclosporin versus colchicine and long-term open study of cyclosporin in Behçet's disease. *Lancet (London, England)*. 1989;1:1093–1096. https://doi.org/10.1016/S0140-6736(89)91098-2.
7 Kaplan MM. New strategies needed for treatment of primary biliary cirrhosis? *Gastroenterology*. 1993;104:651–653. https://doi.org/10.5555/URI:PII:001650859390440N.
8 Gong Y, Gluud C. Colchicine for primary biliary cirrhosis: a cochrane hepato-biliary group systematic review of randomized clinical trials. *Am J Gastroenterol J Gastroenterol*. 2005;100:1876–1885. https://doi.org/10.1111/j.1572-0241.2005.41522.x.
9 McKendry RJ, Kraag G, Seigel S, Al-Awadhi A. Therapeutic value of colchicine in the treatment of patients with psoriatic arthritis. *Ann Rheum Dis*. 1993;52:826–828.
10 Kyle RA, Gertz MA, Greipp PR, et al. A trial of three regimens for primary amyloidosis: colchicine alone, melphalan and prednisone, and melphalan, prednisone, and colchicine. *N Engl J Med*. 1997;336:1202–1207. https://doi.org/10.1056/NEJM199704243361702.
11 Imazio M, Gaita F. Colchicine for cardiovascular medicine. *Future Cardiol*. 2016;12:9–16. https://doi.org/10.2217/fca.15.59.
12 Imazio M, Brucato A, Cemin R, et al. Colchicine for Recurrent Pericarditis (CORP). *Ann Intern Med*. 2011;155:409. https://doi.org/10.7326/0003-4819-155-7-201110040-00359.
13 Weisenberg RC, Broisy GG, Taylor EW. Colchicine-binding protein of mammalian brain and its relation to microtubules. *Biochemistry*. 1968;7:4466–4479. https://doi.org/10.1021/bi00852a043.
14 Seligmann J, Twelves C. Tubulin: an example of targeted chemotherapy. *Future Med Chem*. 2013;5:339–352. https://doi.org/10.4155/fmc.12.217.
15 Katsetos CD, Dráber P. Tubulins as therapeutic targets in cancer: from bench to bedside. *Curr Pharm Des*. 2012;18:2778–2792. https://doi.org/10.2174/138161212800626193.

16 Avendaño C, Menéndez JC. Medicinal Chemistry of Anticancer Drugs. *Amsterdam: Elsevier*. 2008. https://doi.org/10.1016/B978-0-444-52824-7.00001-9.
17 Zhang X, Kong Y, Zhang J, et al. Design, synthesis and biological evaluation of colchicine derivatives as novel tubulin and histone deacetylase dual inhibitors. *Eur J Med Chem*. 2015;95:127–135. https://doi.org/10.1016/J.EJMECH.2015.03.035.
18 Nicolaou KC, Valiulin RA, Pokorski JK, Chang V, Chen JS. Bio-inspired synthesis and biological evaluation of a colchicine-related compound library. *Bioorg Med Chem Lett*. 2012;22:3776–3780. https://doi.org/10.1016/J.BMCL.2012.04.007.
19 Chang D-J, Yoon E-Y, Lee G-B, et al. Design, synthesis and identification of novel colchicine-derived immunosuppressant. *Bioorg Med Chem Lett*. 2009;19:4416–4420. https://doi.org/10.1016/J.BMCL.2009.05.054.
20 Marzo-Mas A, Barbier P, Breuzard G, et al. Interactions of long-chain homologues of colchicine with tubulin. *Eur J Med Chem*. 2017;126:526–535. https://doi.org/10.1016/j.ejmech.2016.11.049.
21 Johnson L, Goping IS, Rieger A, et al. Novel colchicine derivatives and their anti-cancer activity. *Curr Top Med Chem*. 2017;17:2538–2558. https://doi.org/10.2174/1568026617666170104143618.
22 Kumar B, Sharma P, Gupta VP, et al. Synthesis and biological evaluation of pyrimidine bridged combretastatin derivatives as potential anticancer agents and mechanistic studies. *Bioorg Chem*. 2018;78:130–140. https://doi.org/10.1016/J.BIOORG.2018.02.027.
23 Kumar A, Sharma PR, Mondhe DM. Potential anticancer role of colchicine-based derivatives. *Anticancer Drugs*. 2017;28:250–262. https://doi.org/10.1097/CAD.0000000000000464.
24 Shchegravina ES, Maleev AA, Ignatov SK, et al. Synthesis and biological evaluation of novel non-racemic indole-containing allocolchicinoids. *Eur J Med Chem*. 2017;141:51–60. https://doi.org/10.1016/j.ejmech.2017.09.055.
25 Bartusik D, Tomanek B, Lattová E, Perreault H, Tuszynski J, Fallone G. Derivatives of thiocolchicine and its applications to CEM cells treatment using 19F Magnetic Resonance ex vivo. *Bioorg Chem*. 2010;38:1–6. https://doi.org/10.1016/j.bioorg.2009.10.002.
26 Raspaglio G, Ferlini C, Mozzetti S, et al. Thiocolchicine dimers: a novel class of topoisomerase-I inhibitors. *Biochem Pharmacol*. 2005;69:113–121. https://doi.org/10.1016/j.bcp.2004.09.004.
27 Kozaka T, Nakagawa-Goto K, Shi Q, et al. Antitumor agents 273. Design and synthesis of N-alkyl-thiocolchicinoids as potential antitumor agents. *Bioorg Med Chem Lett*. 2010;20:4091–4094. https://doi.org/10.1016/j.bmcl.2010.05.081.
28 Nakagawa-Goto K, Chen CX, Hamel E, et al. Antitumor agents. Part 236: Synthesis of water-soluble colchicine derivatives. *Bioorg Med Chem Lett*. 2005;15:235–238. https://doi.org/10.1016/J.BMCL.2004.07.098.
29 Yasobu N, Kitajima M, Kogure N, et al. Design, synthesis, and antitumor activity of 4-halocolchicines and their pro-drugs activated by cathepsin B. *ACS Med Chem Lett*. 2011;2:348–352. https://doi.org/10.1021/ml100287y.
30 Nishiyama H, Ono M, Sugimoto T, et al. Synthesis and biological evaluation of 4-chlorocolchicine derivatives as potent anticancer agents with broad effective dosage ranges. *Medchemcomm*. 2012;3:1500. https://doi.org/10.1039/c2md20250f.
31 Huczyński A, Rutkowski J, Popiel K, et al. Synthesis, antiproliferative and antibacterial evaluation of C-ring modified colchicine analogues. *Eur J Med Chem*. 2014;90:296–301. https://doi.org/10.1016/j.ejmech.2014.11.037.
32 Huczyński A, Majcher U, Maj E, et al. Synthesis, antiproliferative activity and molecular docking of Colchicine derivatives. *Bioorg Chem*. 2016;64:103–112. https://doi.org/10.1016/j.bioorg.2016.01.002.
33 Majcher U, Klejborowska G, Moshari M, et al. Antiproliferative activity and molecular docking of novel double-modified colchicine derivatives. *Cells*. 2018;7:192. https://doi.org/10.3390/cells7110192.
34 Majcher U, Klejborowska G, Kaik M, et al. Synthesis and biological evaluation of novel triple-modified colchicine derivatives as potent tubulin-targeting anticancer agents. *Cells*. 2018;7:216. https://doi.org/10.3390/cells7110216.
35 Majcher U, Urbaniak A, Maj E, et al. Synthesis, antiproliferative activity and molecular docking of thiocolchicine urethanes. *Bioorg Chem*. 2018;81:553–566. https://doi.org/10.1016/J.BIOORG.2018.09.004.
36 Kurek J, Kwaśniewska-Sip P, Myszkowski K, et al. 7-Deacetyl-10-alkylthiocolchicine derivatives-new compounds with potent anticancer and fungicidal activity. *Medchemcomm*. 2018;9:1708–1714. https://doi.org/10.1039/C8MD00352A.
37 Alkadi H, Khubeiz MJ, Jbeily R. Colchicine: a review on chemical structure and clinical usage. *Infect Disord - Drug Targets*. 2018;18:105–121. https://doi.org/10.2174/1871526517666171017114901.
38 Ghawanmeh AA, Chong KF, Sarkar SM, Bakar MA, Othaman R, Khalid RM. Colchicine prodrugs and codrugs: chemistry and bioactivities. *Eur J Med Chem*. 2018;144:229–242. https://doi.org/10.1016/J.EJMECH.2017.12.029.
39 Ghawanmeh AA, Al-bajalan HM, Mackeen MM, Alali FQ, Chong KF. Recent developments on (−)-colchicine derivatives: synthesis and structure-activity relationship. *Eur J Med Chem*. 2019;111788. https://doi.org/10.1016/j.ejmech.2019.111788.
40 Gracheva IA, Shchegravina ES, Schmalz G, Beletskaya IP, Fedorov AY. Colchicine alkaloids, and synthetic analogues. *Curr Progr Perspectives*. 2020. https://doi.org/10.1021/acs.jmedchem.0c00222.
41 Brossi A, Sharma PN, Atwell L, et al. Biological Effects of Modified Colchicines. 2. Evaluation of Catecholic Colchicines. *Colchifolines, Colchicide, and Novel N-Acyl- and N- Aroyldeacetylcolc hicines*. 1972;1983:1365–1369.
42 Kerekes P, Sharma PN, Brossi A, Chignell CF, Quinni FR. Synthesis and Biological Effects of Novel Thiocolchicines. 3. Evaluation. 1985:1204-1208.
43 Sun L, Hamel E, Lin CM, Hastie SB, Pyluck A, Lee KH. Antitumor Agents. 141. Synthesis and Biological Evaluation of Novel Thiocolchicine Analogs: N-Acyl-, N-Aroyl-, and N-(Substituted benzyl)deacetylthiocolchicines as Potent Cytotoxic and Antimitotic Compounds. *J Med Chem*. 1993;36:1474–1479. https://doi.org/10.1021/jm00062a021.
44 Klejborowska G, Moshari M, Maj E, et al. Synthesis, antiproliferative activity, and molecular docking studies of 4-chlorothiocolchicine analogues. *Chem Biol Drug Des*. 2020;95:182–191. https://doi.org/10.1111/cbdd.13618.
45 Klejborowska G, Urbaniak A, Maj E, et al. Synthesis, biological evaluation and molecular docking studies of new amides of 4-chlorothiocolchicine as anticancer agents. *Bioorg Chem*. December 2019;2020(97):103664. https://doi.org/10.1016/j.bioorg.2020.103664.
46 Klejborowska G, Urbaniak A, Preto J, et al. Synthesis, biological evaluation and molecular docking studies of new amides of 4-bromothiocolchicine as anticancer agents. *Bioorganic Med Chem*. 2019;27:115144. https://doi.org/10.1016/j.bmc.2019.115144.
47 Skehan P, Storeng R, Scudiero D, et al. New colorimetric cytotoxicity assay for anticancer-drug screening. *J Natl Cancer Inst*. 1990;82:1107–1112.
48 Nevozhay D. Cheburator software for automatically calculating drug inhibitory concentrations from in vitro screening assays. Quintas LEM, ed. *PLoS One*. 2014;9:e106186. https://doi.org/10.1371/journal.pone.0106186.
49 Jordan MA, Wilson L. Microtubules as a target for anticancer drugs. *Nat Rev Cancer*. 2004;4:253–265. https://doi.org/10.1038/nrc1317.
50 Delgado M, Urbaniak A, Chambers TC. Contrasting effects of microtubule destabilizers versus stabilizers on induction of death in G1 phase of the cell cycle. *Biochem Pharmacol*. 2019;162:213–223. https://doi.org/10.1016/j.bcp.2018.12.015.
51 Jänicke RU, Sprengart ML, Wati MR, Porter AG. Caspase-3 is required for DNA fragmentation and morphological changes associated with apoptosis. *J Biol Chem*. 1998;273:9357–9360. https://doi.org/10.1074/JBC.273.16.9357.
52 Antoszczak M, Urbaniak A, Delgado M, et al. Biological activity of doubly modified salinomycin analogs – evaluation in vitro and ex vivo. *Eur J Med Chem*. 2018;156:510–523. https://doi.org/10.1016/J.EJMECH.2018.07.021.
53 Urbaniak A, Delgado M, Antoszczak M, Huczyński A, Chambers TC. Salinomycin derivatives exhibit activity against primary acute lymphoblastic leukemia (ALL) cells in vitro. *Biomed Pharmacother*. 2018;99:384–390. https://doi.org/10.1016/J.BIOPHA.2018.01.081.
54 Morris PG, Fornier MN. Microtubule active agents: Beyond the taxane frontier. *Clin Cancer Res*. 2008;14:7167–7172. https://doi.org/10.1158/1078-0432.CCR-08-0169.
55 Leandro-García LJ, Leskelä S, Landa I, et al. Tumoral and tissue-specific expression of the major human ??-tubulin isotypes. *Cytoskeleton*. 2010;67:214–223. https://doi.org/10.1002/cm.20436.
56 Mons S, Veretout F, Carlier MF, et al. The interaction between lipid derivatives of colchicine and tubulin: Consequences of the interaction of the alkaloid with lipid membranes. *Biochim Biophys Acta - Biomembr*. 2000;1468:381–395. https://doi.org/10.1016/S0005-2736(00)00279-0.
57 Shi Q, Verdier-Pinard P, Brossi A, Hamel E, Lee KH. Antitumor Agents-CLXXV. Anti-tubulin action of (+)-thiocolchicine prepared by partial synthesis. *Bioorg Med Chem*. 1997;5:2277–2282. https://doi.org/10.1016/S0968-0896(97)00171-5.
58 Nijmeijer BA, Szuhai K, Goselink HM, et al. Long-term culture of primary human lymphoblastic leukemia cells in the absence of serum or hematopoietic growth factors. *Exp Hematol*. 2009;37:376–385. https://doi.org/10.1016/j.exphem.2008.11.002.
59 Kothari A, Hittelman WN, Chambers TC. Cell cycle-dependent mechanisms underlie vincristine-induced death of primary acute lymphoblastic leukemia cells. *Cancer Res*. 2016;76:3553–3561. https://doi.org/10.1158/0008-5472.CAN-15-2104.
60 Dirks WG, MacLeod RAF, Nakamura Y, et al. Cell line cross-contamination initiative: An interactive reference database of STR profiles covering common cancer cell lines. *Int J Cancer*. 2010;126:303–304. https://doi.org/10.1002/ijc.24999.
61 Alley MC, Scudiero DA, Monks A, et al. Feasibility of drug screening with panels of human tumor cell lines using a microculture tetrazolium assay. *Cancer Res*. 1988;48:589–601.
62 Trott O, Olson AJ. AutoDock Vina: Improving the speed and accuracy of docking with a new scoring function, efficient optimization, and multithreading. *J Comput Chem*. 2009;31:455–461. https://doi.org/10.1002/jcc.21334.